Available online at www.sciencedirect.com
SCIENCE DIRECT®
ELSEVIER
International Journal of Multiphase Flow 31 (2005) 675–705
International Journal of Multiphase Flow
www.elsevier.com/locate/ijmulflow

Volume averaging for the analysis of turbulent spray flows

William A. Sirignano *

Department of Mechanical and Aerospace Engineering, University of California, Irvine, 4200 Engineering Gateway, Room 3202, Irvine, CA 92697-3975, United States

Received 10 July 2004; received in revised form 27 February 2005

Abstract

Spray flow calculations are usually based upon equations that have been developed by averaging droplet properties locally throughout the flow field. Presently, standard procedure for LES (large-eddy simulations) is to average these averaged equations once again to filter the short-length-scale fluctuations. In this paper, the theoretical foundations for the averaged spray equations are examined; then the volume-averaging process for LES and the volume-averaging process for two-phase flows are unified for the analysis of turbulent, two-phase flows. Comments are provided on the relationship between the averaging volume and the computational-cell volume. This paper provides generality to the weighting-function choice in the averaging process and precision to the definition of the volume over which the averaging is performed. New flux terms that result from the averaging process and appear in the governing averaged partial differential equations are identified and their modelling is discussed. Situations are identified where sufficient stratification of properties on the scale smaller than the averaging volume leads to the significance of these quantities. Evolution equations for averaged entropy and averaged vorticity are developed. The relationship amongst the curl of the average gas-phase velocity, the average of the gas-phase-velocity curl, and the rotation of the discrete droplets or particles is established. The needs and challenges for sub-grid modelling to account for small-vortex/droplet interactions are presented. Applications to spray combustion are discussed.

Keywords: Two-phase flow; Particle-laden flow

* Tel.: +1 949 824 3700; fax: +1 949 824 3773.
E-mail address: sirignan@uci.edu

0301-9322/$ - see front matter
doi:10.1016/j.ijmultiphaseflow.2005.02.005

1. Introduction

In both laminar and turbulent spray flow computations that relate to practical situations, it is usual to have flow regions with many more droplets than the achievable number of computational cells. Therefore, we normally define an "average" droplet for each locality that has properties which are representative of the droplets in its neighborhood. Although the volume defining the neighborhood for droplet-property averaging is arbitrary, it is rational to make the averaging volume of the order of the computational-cell volume; resolution is lost by both the averaging process and the computational discretization, so resolution is not gained by making one scale smaller than the other. The length scale for the averaging volume (and therefore for the computational mesh) should be orders of magnitude larger than the droplet diameter or the average spacing between droplets. If each of these droplet length scales were at least an order of magnitude larger than the mesh size, the fields within and around the droplets can be resolved; so there is no point in using average quantities. If the droplet scales and mesh size were comparable, very few droplets are involved in the averaging process and very large fluctuations in the average quantities can be expected.

After this averaging, we have two continua overlaying each other. The two-phase-flow equations have been in use for decades, especially for sprays; see the overviews by Spalding (1980) and Sirignano (1972, 1986, 1999). They were first used by Crocco and Cheng (1956) and Crocco et al. (1962) in the study of combustion instability in liquid-propellant rocket motors. Williams (1962, 1985) presented a derivation of these equations using droplet distribution functions. Both gas and liquid properties are averaged over a neighborhood so that, regardless of whether liquid or gas exists at a particular point in space at a particular instant, both gas-averaged properties and liquid-averaged properties will have continuous values at that point and instant. If we categorize our droplets into many classes (determined for example by initial size, velocity, or composition or by point of injection) and average over each class, there will be a separate continuum for each class plus a continuum for the gas. This is named a multi-continua approach (Sirignano, 1999). The gas-phase continuum is normally solved using an Eulerian formulation for the governing equations while either Lagrangian or Eulerian formulations have been employed for the droplet equations.

The dynamical and thermal behavior of the liquid internal to the droplets, the gas films surrounding the droplets, and the gas regions between neighboring droplets cannot be resolved by solely computational means since they occur on sub-grid scales. So, modelling of those sub-grid phenomena is required. A discussion of the extensive literature on models for droplet dynamics, heating, and vaporization can be found in Sirignano (1999).

Spray flow science can be considered as part of a broader science named two-phase flows which includes additionally suspensions, bubbly flows, dusty flows, and porous flows. Overviews of this field can be found in Soo (1967), Wallis (1969), Marble (1970), Bear (1972) and Drew (1983). Various portions of our analysis will resemble or reproduce elements in the literature; however, significant distinctions occur because of the attempt here to unify the averaging method for two-phase flows with averages constructed for turbulent flows and for computational purposes and because of the special distinctions of rapidly vaporizing, high-liquid-mass sprays. Our interest in sprays is primarily related to liquid–fuel combustion which has some characteristics (Sirignano, 1999) that demand special analytical treatment: the mass and momentum of the liquid (discrete

phase) can be within an order of magnitude of the values for the gas (continuous phase) although the volume fraction of liquid is orders of magnitude smaller; the vaporization time scale in the high-temperature environment can be as small as or smaller than the times for the liquid droplets to reach kinematic or thermal equilibrium with the gas; the Reynolds number (and Peclet number) based on relative gas-droplet velocity and droplet dimension can be of O(10) to O(100) causing substantial stratification and large gradients within the gaseous microstructure surrounding droplets thereby requiring more information than mere averages of the microstructure field; droplet vaporization and heating rates can depend on internal spatial and temporal variations of liquid temperature, composition, and velocity thereby requiring more resolution than simply average properties; and the smallest turbulent length scales can be as small as the droplet size. In the applications of interest, the exchanges of mass, momentum, and energy between the phases will all have highly significant impacts.

Important contributions to the theory of averaging for two-phase flows can be found in the papers of Gray and Lee (1977), Prosperetti and Jones (1984), Zhang and Prosperetti (1994a,b, 1997), Bulthuis et al. (1995) and Prosperetti and Zhang (1995). A discussion emphasizing vaporizing sprays is given by Sirignano (1999). Drew and Passman (1999) give a very broad and detailed overview of averaging methods for multi-component flows; they discuss ensemble-averaging by various methods: constructing a large number of realizations, volume-averaging, and time-averaging. For our purposes, volume averaging has some critical advantages and will be used. Since spatial averaging or filtering methods are widely used by the turbulence community in their large eddy simulations (LES), the treatment of turbulent spray flows integrates better with those studies if spatial averaging is used. Furthermore, we will be interested in unsteady flows so time averaging will not be useful. Finally, we ultimately will solve difference equations rather than differential equations. Finite-volume methods involve averaging over the computational-cell volume and its surfaces. In other numerical differencing methods there is an implied spatial averaging; so, if we used another averaging method for the two-phase character, we are effectively applying two averages to the equations with no particular gain.

Important developments in large-eddy simulations (LES) and so-called ''direct numerical simulations'' (DNS) for particle-laden turbulent flows have been made in recent years. See Squires and Eaton (1991), Elghobashi and Truesdell (1992, 1993), Wang and Squires (1996), Boivin et al. (1998), Druzhinin and Elghobashi (1998, 2001), and Ferrante and Elghobashi (2003). Useful overviews of LES methods for single-phase flows are provided by Piomelli (1999) and Givi (2003). Some recent applications of LES methodology to spray combustion problems are addressed by Sankaran and Menon (2002a,b). The turbulent-flow community is well aware of the important relationship between the volume of the computational cell and the length scales for the phenomena which are filtered or averaged.

Generally, the literature on the development of the averaged equations for two-phase flows (Sirignano, 1999; Gray and Lee, 1977; Prosperetti and Jones, 1984) has not been specific about the volume size or shape to define the neighborhood over which averaging occurs. In particular, the relationship between the averaging process for multi-fluid flows and the high-wavenumber filtering process for turbulent flows, as well as the relationship between the computational-cell shape and size and the shape and size of the averaging volume, have not been well treated yet. Nor has the error been fully evaluated for the common gas-phase approximation that the volume average of a product equals the product of the volume averages; the impact of this on

highly-stratified-flow microstructures will be shown to have potential importance. A substantial amount of research by Prosperetti and co-workers (Zhang and Prosperetti, 1994a,b, 1997; Bulthuis et al., 1995; Prosperetti and Zhang, 1995) is based upon multi-realization ensemble averaging rather than volume averaging. The literature on LES for single-phase flows (Piomelli, 1999; Givi, 2003) also discusses the process of averaging over a neighborhood to create a new continuum and modified governing equations. They tend to refer to the averaging process as a "filtering" process since they filter out the portion of the spectrum associated with smaller length scales. In principle, of course, averaging and filtering are the same here. The spray researchers can learn from the LES researchers who do address the specification of the averaging-volume size and shape and the modelling and evaluation of the difference between the average of a product and the product of the averages. Here, we will attempt to make that advance first for laminar spray flows and then for turbulent spray flows.

Researchers have begun to treat turbulent spray and particle-laden flows using either LES or DNS. Particle-, droplet-, or bubble-laden flows in cases of homogeneous turbulence (Elghobashi and Truesdell, 1992, 1993; Boivin et al., 1998; Druzhinin and Elghobashi, 1998; Ferrante and Elghobashi, 2003), temporal mixing layers (Ling et al., 1999), and spatially developing mixing layers (Druzhinin and Elghobashi, 2001) have been treated by DNS. The LES approach has been used for turbulent, particle-laden channel flow (Wang and Squires, 1996) and turbulent combustion (Sankaran and Menon, 2002a,b). Both DNS and LES analyses typically begin with equations that treat the droplet and gas properties as continuous variables. So, an implicit averaging has been made on the droplet scale. Then, for LES, another averaging (or filtering) is performed explicitly to avoid resolution of the smallest scales of turbulence. The modelling of the droplet behavior has neglected any direct interaction of small eddies with the droplets. Rather, the resulting equations are based implicitly on the assumption that the smallest eddies of the turbulence are larger than the largest droplet scales. Here, we will attempt to unify the droplet averaging process and the LES length-scale filtering process into one process. We will discuss the implications of the situation where the smallest eddy scales are comparable to the droplet scales.

The so-called DNS calculation of spray or particle-laden flows is also built upon modified equations for the flow. (For that reason, this author finds the "DNS" label inappropriate for its current use in two-phase flow calculations.) Whether the droplets are averaged together as a group and represented by an average droplet or they are represented individually as point (monopole) sources, there is a loss of resolution on the scale of the droplet and its surrounding film. So, the "DNS" calculations require modelling of the behavior at the droplet scales and implicitly are restricted to situations where the smallest eddy scales are at least an order magnitude larger than the droplet scales. Many interesting situations, particularly in practical combustors, involve comparable sizes for droplet scales and the Kolmogorov scale of turbulence. For these situations, current "DNS" and LES methods would both be inadequate.

Recent work by Archambault et al. (2003a,b) extends the probability density function approach of Williams (1962, 1985). It differs from the approach of this paper in that it relies on multi-realization ensembles thereby not unifying LES and two-phase-flow averaging processes. Also, it neglects the effects of heat and mass exchanges between the phases.

The next section presents the basic equations governing the gas and liquid phases of the flow. Then, the averaging process is defined and the averaged equations are developed for each phase. The liquid-phase equations are also presented in Lagrangian form. Computational implications

are discussed. In the following section, certain newly identified (at least within the spray literature) flux terms in the equations, each related to the difference between an average of a product and a product of the averages, are analyzed and quantified using simplistic models of the flow on the scale smaller than that of the averaging volume (i.e., sub-grid scale or microstructural scale). The microstructural behavior and analytical challenge are discussed for laminar flows, for flows where the smallest turbulent eddy is larger than the microstructure, and for flows where the smallest turbulent eddies appear in the microstructure.

2. Development of the averaged equations

2.1. The primitive equations

The primitive equations are the well known conservation equations for a multi-component, chemically reacting, unsteady, three-dimensional gas phase. The overall gas-phase continuity equation is

$$\frac{\partial \rho}{\partial t} + \frac{\partial(\rho u_j)}{\partial x_j} = 0 \tag{1}$$

ρ, u_i, t, and x_i are the density, ith component of velocity, time, and ith Cartesian space coordinate, respectively. The species continuity equation for any of the N gaseous species can be written as

$$\frac{\partial(\rho Y_n)}{\partial t} + \frac{\partial(\rho Y_n u_j)}{\partial x_j} + \frac{\partial(\rho Y_n V_{n,j})}{\partial x_j} = \rho \omega_n, \quad n = 1, \ldots, N \tag{2}$$

Y_n, $V_{n,i}$ and ω_n are the mass fraction, ith component of mass-diffusion velocity, and the chemical reaction rate, respectively, for the nth species. For cases where Fickian diffusion can be assumed for multi-component diffusion in a gas dominated by one particular species (e.g., nitrogen), we have

$$V_{n,i} = -\frac{D_n}{Y_n}\frac{\partial Y_n}{\partial x_i} \tag{3}$$

where D_n is the mass diffusivity for the nth species. The momentum equation is

$$\frac{\partial(\rho u_i)}{\partial t} + \frac{\partial(\rho u_i u_j)}{\partial x_j} + \frac{\partial p}{\partial x_i} = \frac{\partial \tau_{ij}}{\partial x_j} + \rho g_i \tag{4}$$

p, τ_{ij}, and g_i are the pressure, viscous stress tensor, and ith component of the gravitational acceleration, respectively. The following form of the energy equation will be used:

$$\frac{\partial(\rho h)}{\partial t} + \frac{\partial(\rho h u_j)}{\partial x_j} + \frac{\partial q_j}{\partial x_j} = \frac{\partial p}{\partial t} + u_j \frac{\partial p}{\partial x_j} + \Phi + \sum_{n=1}^{N} \rho \omega_n Q_n \tag{5}$$

where h is the specific enthalpy, Q_n is the chemical heating value (simply the negative of the heat of formation) of the nth species, and the viscous dissipation and the heat-flux vector are given by

$$\Phi = \tau_{ij}\frac{\partial u_i}{\partial x_j} \tag{6}$$

and

$$q_i = -\lambda\frac{\partial T}{\partial x_i} + q_{\mathrm{rad},i} + \sum_{n=1}^{N}\rho V_{n,i}h_n Y_n \tag{7}$$

The quantities λ, T, $q_{\mathrm{rad},i}$, and h_n represent the thermal conductivity, temperature, radiative heat flux, and specific enthalpy of species n, respectively. So, the first term in Eq. (7) is the Fourier heat conduction while the third term is the heat flux created by the mass diffusion of species with differing specific heats.

We will consider a perfect gas so that

$$p = \rho RT \tag{8}$$

where R is the gas "constant" that actually can vary in a multi-component flow due to its molecular-weight and mass-fraction dependencies.

The combined First and Second Laws of Thermodynamics lead to a differential relationship for an element of mass, Williams (1985); $T\,\mathrm{d}s = \mathrm{d}h - (1/\rho)\,\mathrm{d}p - \sum_{n=1}^{N} e_n\,\mathrm{d}Y_n$ where s is the specific entropy and e_n is the internal energy (without the energy of formation) of the nth species. Note that the last term on the right side goes to zero when the specific heats of all species have the same value at any given temperature. This equation can be recast in terms of Lagrangian time derivatives following the mass element and combined with Eqs. (1) and (5) to yield

$$\begin{aligned}\rho\left\{\frac{\partial s}{\partial t} + u_j\frac{\partial s}{\partial x_j}\right\} &= \frac{\partial(\rho s)}{\partial t} + \frac{\partial(\rho u_j s)}{\partial x_j} = \frac{p}{T}\frac{\partial u_j}{\partial x_j} + \frac{\rho c_v}{T}\left\{\frac{\partial T}{\partial t} + u_j\frac{\partial T}{\partial x_j}\right\}\\ &= \frac{1}{T}\left\{-\frac{\partial q_j}{\partial x_j} + \Phi + \sum_{n=1}^{N}\rho\omega_n[Q_n - e_n] + \sum_{n=1}^{N} e^n\frac{\partial(\rho V_{n,j}Y_n)}{\partial x_j}\right\} \overset{\mathrm{def}}{=} \frac{R_1}{T}\end{aligned} \tag{9}$$

In the special case where the specific heats of all species have the same value, the simplification results that

$$\frac{R_1}{T} = \frac{1}{T}\left\{-\frac{\partial q_j}{\partial x_j} + \Phi + \sum_{n=1}^{N}\rho\omega_n Q_n\right\} \tag{10}$$

The same Eqs. (1)–(9) will apply for the liquid phase with the exceptions that ω_n, for any liquid-phase species, and $q_{\mathrm{rad},i}$ will be zero and liquid density will be constant. The set of N species will include any species which appears in at least of one of the two phases. The liquid-phase dependent variables will carry a special subscript to distinguish them from the gas-phase variables. We will have, for example, $u_{l,i}$, ρ_l, $Y_{l,n}$, $V_{l,n,i}$, p_l, $\tau_{l,ij}$, h_l, $q_{l,i}$, Φ_l, T_l, and $h_{l,n}$.

2.2. Averaging of dependent variables

Let us consider the variable $\theta(\vec{x}, t)$ to have a value of unity in the gas phase and zero in the liquid phase. θ has been named a characteristic function or a component indicator function (Drew

and Passman, 1999). The function was introduced as a void-volume-distribution function in a series of papers on porous flows (Whitaker, 1966, 1967) that used volume averaging over the microstructure that included both the solid porous material and the fluid in the pores. A spatial derivative of θ is therefore zero everywhere except at a liquid/gas interface where it is a Dirac delta function. Note that the time derivative will be zero except at a moving interface. We now define a weighting factor $G(\vec{x}-\vec{\xi})$ for the averaging of quantities over the neighborhood of any particular point $\vec{x}$ at any particular instant t; $\vec{\xi}$ varies to identify the points in the neighborhood of the point $\vec{x}$. $\vec{x}$ and $\vec{\xi}$ have the same reference origin so that $\vec{x}-\vec{\xi}$ is a relative position. G depends only on the relative position; it does not separately depend on $\vec{x}$ or $\vec{\xi}$. Nor does it have a temporal dependence. We also require that

$$\int_{-\infty}^{\infty}\int_{-\infty}^{\infty}\int_{-\infty}^{\infty} G(\vec{x}-\vec{\xi})\,\mathrm{d}\vec{\xi} = 1 \tag{11}$$

where $\mathrm{d}\vec{\xi} \overset{\text{def}}{=} \mathrm{d}\xi_1\,\mathrm{d}\xi_2\,\mathrm{d}\xi_3$. Three examples of symmetric choices for G are

$$G \overset{\text{def}}{=} \begin{cases} \frac{3}{4\pi a^3} & \text{if } 0 \leqslant |\vec{x}-\vec{\xi}| \leqslant a \\ 0 & \text{if } |\vec{x}-\vec{\xi}| > a \end{cases} \tag{12}$$

$$G \overset{\text{def}}{=} \begin{cases} \frac{1}{8abc} & \text{if } -a \leqslant x_1 \leqslant a; -b \leqslant x_2 \leqslant b; -c \leqslant x_3 \leqslant c \\ 0 & \text{if otherwise} \end{cases} \tag{13}$$

and

$$G \overset{\text{def}}{=} \frac{1}{2}\left(\frac{b}{\pi}\right)^{3/2} e^{-b|\vec{x}-\vec{\xi}|^2} \tag{14}$$

In the choice presented by Eq. (12) or (13), the spherical or rectangular volume is named the averaging volume. In the choice given by Eq. (14), the integration should be performed over the infinite domain. If the exponential function is "clipped" to become zero outside of some finite symmetrical domain (such as a sphere or rectangular box) centered at the point $\vec{x}$, the constants in the G function must be adjusted to satisfy Eq. (11). The domain where the clipped G is positive is named the averaging volume for this case. One could proceed with an infinite averaging volume but, as we noted, there is disadvantage in making the averaging volume larger than the computational cell volume. The choice of Eq. (13) is commonly used for LES computations and fits well with a rectangular gridding scheme.

Note that, in the above examples, two types of symmetry are displayed for the function G: for spherical symmetry, $G(|\vec{x}-\vec{\xi}|) = G(|\vec{\xi}-\vec{x}|)$ while, for symmetry about each of three orthogonal planes, $G(x_1-\xi_1, x_2-\xi_2, x_3-\xi_3) = G(\xi_1-x_1, x_2-\xi_2, x_3-\xi_3)$, $G(x_1-\xi_1, x_2-\xi_2, x_3-\xi_3) = G(x_1-\xi_1, \xi_2-x_2, x_3-\xi_3)$, and $G(x_1-\xi_1, x_2-\xi_2, x_3-\xi_3) = G(x_1-\xi_1, x_2-\xi_2, \xi_3-x_3)$. In the following analyses, the results still apply for either symmetry type. Furthermore, the condition of symmetry of G is not required. The results in this paper would still apply, for example, if the point $\vec{x}$ were not in the center of the averaging volume or if the averaging volume had a non-symmetric shape.

$G(\vec{x}-\vec{\xi})$ has three important properties that will be useful in this analysis. They apply for either symmetric or asymmetric G functions. One is the condition that $\partial G/\partial x_i = -\partial G/\partial \xi_i$. This condition

will be valuable in determining the average value of a spatial gradient. Another property is that $G \to 0$ as $|\vec{x} - \vec{\xi}| \to \infty$. The third property is that it has units of reciprocal volume (reciprocal length cubed) and is normalized so that, when used as a weighting factor in an integration over the volume, it maintains the proper dimensional units and implicitly divides the integral by the weighted volume. The importance of the constraints on the choice of G has been well recognized by researchers in the LES field but not as well recognized by two-phase flow researchers. Define the void volume (fraction of volume occupied by gas) as

$$\overline{\theta(\vec{x},t)} \stackrel{\text{def}}{=} \int_{-\infty}^{\infty}\int_{-\infty}^{\infty}\int_{-\infty}^{\infty} G(\vec{x}-\vec{\xi})\theta(\vec{\xi},t)\,\mathrm{d}\vec{\xi} \tag{15}$$

The overbar implies an average over the volume. Clearly, the volume fraction occupied by liquid will be

$$\overline{1-\theta(\vec{x},t)} = 1 - \overline{\theta(\vec{x},t)} = \int_{-\infty}^{\infty}\int_{-\infty}^{\infty}\int_{-\infty}^{\infty} G(\vec{x}-\vec{\xi})(1-\theta(\vec{\xi},t))\,\mathrm{d}\vec{\xi} \tag{16}$$

In averaging the gas-phase flow variables, some variables will be averaged with normalized density in the weighting factor while others will be averaged without the use of density. The choice of whether or not to use density weighting for any particular variable here follows conventional practice, is intended to produce the simpler form of the averaged equations, and is based upon how the specific term appears in the governing equations. When density-weighting is used, the averaging is over the mass rather than simply the volume; this is known as Favre-averaging. Note that the two types of averaging (volume and Favre) produce identical results for the situation where density is uniform such as we shall see later for the averaged liquid-phase equations.

The average gas density will be

$$\overline{\rho(\vec{x},t)} \stackrel{\text{def}}{=} \int_{-\infty}^{\infty}\int_{-\infty}^{\infty}\int_{-\infty}^{\infty} G(\vec{x}-\vec{\xi})\theta(\vec{\xi},t)\rho(\vec{\xi},t)\,\mathrm{d}\vec{\xi} \tag{17}$$

The scalars Y_n, h, and ω_n and the vector u_i are averaged with a mass (Favre) weighting. If ψ is a generic scalar or vector, we obtain

$$\overline{\rho(\vec{x},t)\psi(\vec{x},t)} \stackrel{\text{def}}{=} \overline{\rho(\vec{x},t)}\langle\psi(\vec{x},t)\rangle \stackrel{\text{def}}{=} \int_{-\infty}^{\infty}\int_{-\infty}^{\infty}\int_{-\infty}^{\infty} G(\vec{x}-\vec{\xi})\theta(\vec{\xi},t)\rho(\vec{\xi},t)\psi(\vec{\xi},t)\,\mathrm{d}\vec{\xi} \tag{18}$$

Here, the brackets $\langle\ \rangle$ will be used below to denote a mass-weighted average of a property or of the product of properties. Now, consider $\rho Y_n u_i$, $\rho Y_n V_{n,i}$, and $\rho h u_i$. If we take the product of a scalar ψ and a vector w_i, we obtain

$$\begin{aligned}\overline{\rho(\vec{x},t)\psi(\vec{x},t)w_i(\vec{x},t)} &\stackrel{\text{def}}{=} \overline{\rho(\vec{x},t)}\langle\psi(\vec{x},t)w_i(\vec{x},t)\rangle \\ &\stackrel{\text{def}}{=} \int_{-\infty}^{\infty}\int_{-\infty}^{\infty}\int_{-\infty}^{\infty} G(\vec{x}-\vec{\xi})\theta(\vec{\xi},t)\rho(\vec{\xi},t)\psi(\vec{\xi},t)w_i(\vec{\xi},t)\,\mathrm{d}\vec{\xi}\end{aligned} \tag{19}$$

The mass-weighted average of the product of two velocity vectors produces the tensor

$$\overline{\rho(\vec{x},t)u_i(\vec{x},t)u_j(\vec{x},t)} \stackrel{\text{def}}{=} \overline{\rho(\vec{x},t)}\langle u_i(\vec{x},t)u_j(\vec{x},t)\rangle \stackrel{\text{def}}{=} \int_{-\infty}^{\infty}\int_{-\infty}^{\infty}\int_{-\infty}^{\infty} G(\vec{x}-\vec{\xi})\theta(\vec{\xi},t)u_i(\vec{\xi},t)u_j(\vec{\xi},t)\,\mathrm{d}\vec{\xi} \tag{20}$$

For variables such as Φ, q_i, p, and the viscous stress tensor τ_{ij}, the averaging is performed with a volume weighting to obtain

$$\overline{\Phi(\vec{x},t)} \stackrel{\text{def}}{=} \int_{-\infty}^{\infty}\int_{-\infty}^{\infty}\int_{-\infty}^{\infty} G(\vec{x}-\vec{\xi})\theta(\vec{\xi},t)\Phi(\vec{\xi},t)\,\mathrm{d}\vec{\xi} \tag{21}$$

$$\overline{q_i(\vec{x},t)} \stackrel{\text{def}}{=} \int_{-\infty}^{\infty}\int_{-\infty}^{\infty}\int_{-\infty}^{\infty} G(\vec{x}-\vec{\xi})\theta(\vec{\xi},t)q_i(\vec{\xi},t)\,\mathrm{d}\vec{\xi} \tag{22}$$

$$\overline{\theta(\vec{x},t)}\widehat{p}(\vec{x},t) \stackrel{\text{def}}{=} \overline{p(\vec{x},t)} \stackrel{\text{def}}{=} \int_{-\infty}^{\infty}\int_{-\infty}^{\infty}\int_{-\infty}^{\infty} G(\vec{x}-\vec{\xi})\theta(\vec{\xi},t)p(\vec{\xi},t)\,\mathrm{d}\vec{\xi} \tag{23}$$

and

$$\overline{\theta(\vec{x},t)}\widehat{\tau}_{ij}(\vec{x},t) \stackrel{\text{def}}{=} \overline{\tau_{ij}(\vec{x},t)} \stackrel{\text{def}}{=} \int_{-\infty}^{\infty}\int_{-\infty}^{\infty}\int_{-\infty}^{\infty} G(\vec{x}-\vec{\xi})\theta(\vec{\xi},t)\tau_{ij}(\vec{\xi},t)\,\mathrm{d}\vec{\xi} \tag{24}$$

The averages for pressure and viscous stress indicated by the "hat" symbol differ from the others with the explicit appearance of $\bar{\theta}$ in order to facilitate below the collection of terms that contribute to the aerodynamic forces on the droplets. In the case of Fickian diffusion, it follows from Eq. (3) that the integral in Eq. (19) becomes the average of the triple product of density ρ, mass diffusivity D, and the gradient of mass fraction $\partial Y_n/\partial x_i$. Furthermore, if the product ρD were constant, the integral becomes the product of ρD and the average gradient.

The average values for the liquid properties are obtained by using the liquid-properties fields and replacing $\theta(\vec{\xi},t)$ by $[1-\theta(\vec{\xi},t)]$ in the integrands of Eqs. (17)–(24). Also, $\overline{\theta(\vec{x},t)}$ is replaced by $[1-\overline{\theta(\vec{x},t)}]$ in Eqs. (23) and (24). For the constant-density liquid considered here, there is no distinction in the results between volume-weighted averages and mass-(Favre-) weighted averages. So, only the overbar is used to indicate liquid-property averages. We will not write those liquid-phase relations here because they are obvious.

The application of boundary conditions will present some problems. The specified value of a flow variable at a boundary is not exactly equal to the average value of that variable in a neighborhood adjacent to the boundary. So, some higher-order error is made when that condition of equality is applied. It will not be a problem if the weighting factor G is non-zero outside of the boundary provided that the flow variables are prescribed to be zero outside of the boundaries.

2.3. Averaging of derivatives

The relationships between the volume average of the derivative of a dependent variable and the derivative of a volume-averaged dependent variable was shown for porous flow problems by Whitaker (1966, 1967) and Slattery (1967). Later, Whitaker (1973) extended the treatment to multiphase systems with mass exchange. In those early works, G was not identified but implicitly was set equal to unity over the averaging volume. The possibility of volume changes with $\vec{x}$ was not considered. The time derivative of any averaged (scalar, vector, or tensor) gas-phase quantity ϕ can be related to the average of the time derivative as

$$\overline{\frac{\partial \phi(\vec{x},t)}{\partial t}} = \int_{-\infty}^{\infty}\int_{-\infty}^{\infty}\int_{-\infty}^{\infty} G(\vec{x}-\vec{\xi})\theta(\vec{\xi},t)\frac{\partial \phi(\vec{\xi},t)}{\partial t}\,\mathrm{d}\vec{\xi}$$
$$= \frac{\partial}{\partial t}\int_{-\infty}^{\infty}\int_{-\infty}^{\infty}\int_{-\infty}^{\infty} G(\vec{x}-\vec{\xi})\theta(\vec{\xi},t)\phi(\vec{\xi},t)\,\mathrm{d}\vec{\xi}$$
$$- \int_{-\infty}^{\infty}\int_{-\infty}^{\infty}\int_{-\infty}^{\infty} G(\vec{x}-\vec{\xi})\frac{\partial \theta(\vec{\xi},t)}{\partial t}\phi(\vec{\xi},t)\,\mathrm{d}\vec{\xi} \tag{25}$$

So, recognizing that θ will change with time only because droplet motion, distortion, vaporization, or condensation causes the gas/liquid interface to move, we can relate the time derivative of θ to the velocity of the interface as

$$\frac{\partial \theta(\vec{\xi},t)}{\partial t} = -u_{\theta,j}\frac{\partial \theta(\vec{\xi},t)}{\partial \xi_j} \tag{26}$$

where $u_{\theta,i}$ is the ith component of the normal interface velocity. With n taken as the local normal coordinate at the surface, $\partial\theta(\vec{\xi},t)/\partial n$ is a Dirac delta function; so, the three-dimensional integral can immediately be integrated to give a two-dimensional surface integral over all interfaces in the averaging volume. The result is that

$$\overline{\frac{\partial \phi(\vec{x},t)}{\partial t}} = \frac{\partial \overline{\phi(\vec{x},t)}}{\partial t} + \int_S\int G(\vec{x}-\vec{\zeta})\phi(\vec{\zeta},t)u_{\theta,j}(\vec{\zeta},t)\,\mathrm{d}A_j \tag{27}$$

Here, $\mathrm{d}A_i$ is the ith component of the normal interfacial area vector, pointing into the continuous phase (gas), and the $\vec{\zeta}$ vectors are the subset of $\vec{\xi}$ vectors that locate points on the interfaces. In Eqs. (25)–(27), ϕ can be a scalar, vector, or tensor.

Let us now examine the average of a spatial derivative. Again, ϕ can be a scalar, vector, or tensor.

$$\overline{\frac{\partial \phi(\vec{x},t)}{\partial x_i}} = \int_{-\infty}^{\infty}\int_{-\infty}^{\infty}\int_{-\infty}^{\infty} G(\vec{x}-\vec{\xi})\theta(\vec{\xi},t)\frac{\partial \phi(\vec{\xi},t)}{\partial \xi_i}\mathrm{d}\vec{\xi}$$
$$= \int_{-\infty}^{\infty}\int_{-\infty}^{\infty}\int_{-\infty}^{\infty}\frac{\partial[G(\vec{x}-\vec{\xi})\theta(\vec{\xi},t)\phi(\vec{\xi},t)]}{\partial \xi_i}\mathrm{d}\vec{\xi}$$
$$- \int_{-\infty}^{\infty}\int_{-\infty}^{\infty}\int_{-\infty}^{\infty}\frac{\partial G(\vec{x}-\vec{\xi})}{\partial \xi_i}\theta(\vec{\xi},t)\phi(\vec{\xi},t)\,\mathrm{d}\vec{\xi} - \int_{-\infty}^{\infty}\int_{-\infty}^{\infty}\int_{-\infty}^{\infty} G(\vec{x}-\vec{\xi})\frac{\partial \theta(\vec{\xi},t)}{\partial \xi_i}\phi(\vec{\xi},t)\,\mathrm{d}\vec{\xi}$$
$$= 0 + \frac{\partial}{\partial x_i}\int_{-\infty}^{\infty}\int_{-\infty}^{\infty}\int_{-\infty}^{\infty} G(\vec{x}-\vec{\xi})\theta(\vec{\xi},t)\phi(\vec{\xi},t)\,\mathrm{d}\vec{\xi} - \int_S\int G(\vec{x}-\vec{\zeta})\phi(\vec{\zeta},t)\,\mathrm{d}A_i \tag{28}$$

The first integral on the right side is zero because $G \to 0$ as $|\,\vec{x}-\vec{\xi}\,| \to \infty$. So, we have

$$\overline{\frac{\partial \phi(\vec{x},t)}{\partial x_i}} = \frac{\partial \overline{\phi(\vec{x},t)}}{\partial x_i} - \int_S\int G(\vec{x}-\vec{\zeta})\phi(\vec{\zeta},t)\,\mathrm{d}A_i \tag{29}$$

The computational cell in a calculation need not be identical in shape to the averaging volume but should have the same approximate magnitude for volume since the largest volume determines the resolution for the problem. The averaging volume is distinct from the computational volume in

principle since there are an infinite number of averaging volumes (before discretization of the differential equations into difference equations), one corresponding to each point in space, while a finite number of computational cell volumes exist. In other words, averaging volumes can overlap each other while cell volumes cannot. Of course, in practice, there is no advantage to considering more than one point for each computational cell since resolution cannot be improved by consideration of more points. So, after discretization, the number of averaging volumes engaged in the calculation equals the number of cells.

If, for convenience, averaging volumes are made identical to computational cell volumes in uniform-sized Cartesian grids, the averaging-volume shapes can be symmetric types such as the rectangular boxes considered with Eq. (13), all volume sizes would be uniform. However, with non-uniform Cartesian grids, cylindrical or spherical grids, and unstructured grids, including finite elements, the size and shape of the averaging volume would change if it were set equal to the computational cell volume locally. In some situations, the averaging volume might be varied spatially because the computationally resolved, physical-length scales vary. The spatial variation means that $G = G(\vec{x}, \vec{x} - \vec{\xi})$; namely, a separate dependence on $\vec{x}$ appears which modifies the gradient formulation from the form given by Eqs. (28) and (29). An option is to correct Eqs. (28) and (29) and the resulting conservation equations to account for a variation in the averaging volume. For example, suppose we have a non-uniform or unstructured grid and use $G = 1/V$ where V is the averaging volume which is now a function of $\vec{x}$. Then, Eq. (29) is modified to be

$$\overline{\frac{\partial \phi(\vec{x},t)}{\partial x_i}} = \frac{\partial \overline{\phi(\vec{x},t)}}{\partial x_i} + \frac{\partial(\log V)}{\partial x_i}\overline{\phi(\vec{x},t)} - \int_{A^*}\int \phi(\vec{\eta},t)\theta(\vec{\eta},t)\frac{1}{V}\frac{\partial n(\vec{\eta})}{\partial x_i}\,\mathrm{d}A^* - \int_S \int \frac{1}{V}\phi(\vec{\zeta},t)\,\mathrm{d}A_i \tag{30}$$

where A^* is the external surface area of the averaging volume, $\vec{\eta}$ is a vector locating a point on that surface, and n is the positive-outward length extension of that surface locally as V changes with $\vec{x}$. The second and third terms on the right side are the result of the variation in the volume. The second term is caused by the change in the magnitude of G over the volume as Eq. (11) is obeyed. The other term results from the change in the domain of the integration. They can be combined easily into one term when the rate of local volume change is uniform over the bounding surface of the averaging volume. That is, $\partial n/\partial x_i$ is uniform over the surface. Then, we obtain

$$\overline{\frac{\partial \phi(\vec{x},t)}{\partial x_i}} = \frac{\partial \overline{\phi(\vec{x},t)}}{\partial x_i} + \frac{\partial(\log V)}{\partial x_i}\{\overline{\phi(\vec{x},t)} - \overline{\phi_S(\vec{x},t)}\} - \int_S \int \frac{1}{V}\phi(\vec{\zeta},t)\,\mathrm{d}A_i \tag{31}$$

where the average of ϕ over the bounding surface is given by

$$\bar{\phi}_S = \frac{1}{A^*}\int_{A^*}\int \phi(\vec{\eta},t)\theta(\vec{\eta},t)\,\mathrm{d}A^* \tag{32}$$

The new term can be zero in special cases, e.g., when ϕ is uniform over the boundary and equal to $\bar{\phi}$, but generally it is not zero. The problem with this situation is that a model for the value of ϕ on the volume boundary is needed. If the averaging volume were a sphere centered at $\vec{x}$, the use of the mean-value theorem (see p. 276 of Courant and Hilbert, 1962) leads to the conclusion that $\bar{\phi} - \bar{\phi}_S = \mathrm{O}(R^2\nabla^2\phi)$ where R is the sphere radius. This implies that the ratio of the second term

on the right side of Eq. (31) to the first term on that side is $O(R^2/(L_1L_2))$. Here, L_1 is the physical length scale for change in ϕ and L_2 is the designed numerical length scale for change in the averaging volume. We can expect this order of magnitude to remain the same if the averaging volume is not spherical. So, clearly if L_2 is chosen to be too small (i.e., change in volume size is too abrupt) significant errors can occur if the second term on the right side of Eq. (31) is not considered. Note that this need for correction would apply to any calculation with averaging, including single-phase LES calculations as recognized by Ghosal and Moin (1995). There also has been recognition of the potential for error by the computational-fluid-dynamics community. See, for example, pp. 60–63 of the second volume of the book by Fletcher (1991) where non-uniform grids are discussed. It is known that if computational mesh size varies too abruptly with position, errors can be introduced that are of first order in an otherwise second-order-accurate differencing scheme.

Independence of grid size is a necessary condition. For calculations with filtering or averaging, this condition should be interpreted as the requirement that, for two averaging-volume choices with mesh lengths that are of the same order of magnitude (e.g., a factor of two difference is the standard test), the two computations should agree for the portion of the spectrum with length scales larger than the larger of the two filtering lengths for the two choices. That is, only the mutually unfiltered portion can be expected to agree. Clearly, independence of grid size depends not only on the correct choice of grid size but also on the correct choice of sub-grid models, since grid size can quantitatively affect the sub-grid model.

2.4. Averaged gas-phase equations

We will now multiply each one of Eqs. (1), (2), (4), (5) and (8) by the product $G\theta$ and integrate term-by-term over the volume. The relations given by Eqs. (15)–(24), (27) and (29) will be used to substitute for the various integrals. Then, some rearrangement of terms will be made to yield the averaged equations. Finally, we obtain the averaged gas-phase continuity equation

$$\frac{\partial \bar{\rho}}{\partial t} + \frac{\partial(\bar{\rho}\langle u_j\rangle)}{\partial x_j} = \dot{M} \tag{33}$$

and the averaged gas-phase species continuity equation

$$\frac{\partial(\bar{\rho}\langle Y_n\rangle)}{\partial t} + \frac{\partial(\bar{\rho}\langle Y_n\rangle\langle u_j\rangle)}{\partial x_j} + \frac{\partial(\bar{\rho}\langle Y_n\rangle\langle V_{n,j}\rangle)}{\partial x_j} = \bar{\rho}\langle\omega_n\rangle + \dot{M}\epsilon_n + \frac{\partial(\bar{\rho}\alpha_{n,j})}{\partial x_j} + \frac{\partial(\bar{\rho}\beta_{n,j})}{\partial x_j} \quad n = 1,\ldots,N \tag{34}$$

In these equations, we have used the definitions

$$\dot{M} \overset{\text{def}}{=} \int_S \int G(\vec{x}-\vec{\zeta})\rho(\vec{\zeta},t)[u_j(\vec{\zeta},t) - u_{\theta,j}(\vec{\zeta},t)]\,\mathrm{d}A_j \tag{35}$$

$$\dot{M}\epsilon_n \overset{\text{def}}{=} \int_S \int G(\vec{x}-\vec{\zeta})\rho(\vec{\zeta},t)Y_n(\vec{\zeta},t)[u_j(\vec{\zeta},t) - u_{\theta,j}(\vec{\zeta},t) + V_{n,j}(\vec{\zeta},t)]\,\mathrm{d}A_j \tag{36}$$

$$\alpha_{n,i} \overset{\text{def}}{=} \langle Y_n\rangle\langle u_i\rangle - \langle Y_n u_i\rangle \tag{37}$$

$$\beta_{n,i} \stackrel{\text{def}}{=} \langle Y_n \rangle \langle V_{n,i} \rangle - \langle Y_n V_{n,i} \rangle \tag{38}$$

Note that $[u_j(\vec{\zeta},t) - u_{\theta,j}(\vec{\zeta},t)]$ in Eqs. (35) and (36) is the relative velocity of the gas at the liquid surface, so, the normal component of this velocity is the Stefan velocity at the surface caused by the vaporization (or condensation). Therefore, $\dot{M}$ is the total vaporization rate per unit volume due to all of the droplets in the neighborhood. ϵ_n is the fractional vaporization rate of the nth species. Models for $\dot{M}$ and ϵ_n (for situations where the smallest scales of turbulence are larger than the droplet scales) can be found (Sirignano, 1999) and will not be discussed further here. The quantities, $\alpha_{n,i}$ and $\beta_{n,i}$, require modelling and will be discussed later.

A Reynolds-stress term will appear in the momentum equation. It is given as

$$\Gamma_{ij} \stackrel{\text{def}}{=} \langle u_i \rangle \langle u_j \rangle - \langle u_i u_j \rangle \tag{39}$$

With the use of Eq. (15), it can be shown that

$$\frac{\partial \bar{\theta}}{\partial x_i} = -\int_{-\infty}^{\infty}\int_{-\infty}^{\infty}\int_{-\infty}^{\infty} \frac{\partial G(\vec{x}-\vec{\zeta})}{\partial \zeta_i}\theta(\vec{\zeta},t)\,\mathrm{d}\vec{\zeta} = \int_{-\infty}^{\infty}\int_{-\infty}^{\infty}\int_{-\infty}^{\infty} G(\vec{x}-\vec{\zeta})\frac{\partial \theta(\vec{\zeta},t)}{\partial \zeta_i}\mathrm{d}\vec{\zeta}$$
$$= \int_S \int G(\vec{x}-\vec{\zeta})\,\mathrm{d}A_i \tag{40}$$

Now following Prosperetti and Jones (1984), a portion of the terms related to the averaged viscous stress and pressure can be combined to yield F_i, the aerodynamic force (per unit volume) on the droplets,

$$F_i \stackrel{\text{def}}{=} \int_S \int G(\vec{x}-\vec{\zeta})\Big\{[\tau_{ij}(\vec{\zeta},t) - \delta_{ij}p(\vec{\zeta},t)] - [\widehat{\tau}_{ij}(\vec{x},t) - \delta_{ij}\widehat{p}(\vec{x},t)]\Big\}\,\mathrm{d}A_j \tag{41}$$

δ_{ij} is the Kronecker delta symbol. Models for F_i, including models for unsteady effects, can be found in the literature and will not be discussed here. See, for example, Sirignano (1999).

The term representing the momentum exchange between the phases associated with vaporization (condensation) is an integral over the liquid surface of the product of the local vaporization rate per unit area and the velocity of the gas at the surface. If the difference between the liquid velocity and the gas velocity at the surface is small compared to the droplet velocity, this term can be modelled as the product of the global vaporization rate and the average droplet velocity. Even if the velocity difference at the surface is not small compared to the droplet velocity, there should be substantial cancellation from the integration of the relative velocity vector over the closed surfaces of the droplets. Therefore, we have for the vaporization case

$$\int_S \int G(\vec{x}-\vec{\zeta})\rho(\vec{\zeta},t)u_i(\vec{\zeta},t)[u_j(\vec{\zeta},t) - u_{\theta,j}(\vec{\zeta},t)]\,\mathrm{d}A_j = \dot{M}\bar{u}_{l,j} \tag{42}$$

where $\bar{u}_{l,i}$ is the averaged liquid velocity. In the condensation case, $\bar{u}_{l,i}$ should be replaced by $\langle u_i \rangle$. So, the gas-phase momentum equation can be cast as

$$\frac{\partial(\bar{\rho}\langle u_i\rangle)}{\partial t} + \frac{\partial(\bar{\rho}\langle u_i\rangle\langle u_j\rangle)}{\partial x_j} + \bar{\theta}\frac{\partial \hat{p}}{\partial x_i} = \bar{\theta}\frac{\partial \hat{\tau}_{ij}}{\partial x_j} + \bar{\rho}g_i - F_i + \dot{M}\bar{u}_{l,j} + \frac{\partial(\bar{\rho}\Gamma_{ij})}{\partial x_j} \tag{43}$$

In his porous flow analysis, Whitaker (1967) found the $\alpha_{n,i}$ term which he named a dispersion vector. $\beta_{n,i}$ did not appear because Fickian diffusion was assumed. Inertial effects were neglected so the Γ_{ij} term was not developed in the porous-flow analyses. Whitaker (1973) also neglected the inertial effects in the more general multi-phase systems transport study. Most of the terms in these equations have been recognized before for spray flows, bubbly flows, and particle-laden flows (Sirignano, 1999). However, the last two terms in Eq. (34) and the last term in Eq. (43) are new terms for spray flow theory. They have been recognized in turbulent flow theory but we shall see how stratification in the microstructure for laminar two-phase flows can make these terms significant. For the development of the averaged energy equation, we note that the term that gives the rate of energy exchange (per unit volume) with the droplets due to heat conduction, mass transfer, and radiation can be modelled (Sirignano, 1999) as

$$\int_S \int G(\vec{x}-\vec{\zeta})\{\rho(\vec{\zeta},t)h(\vec{\zeta},t)[u_j(\vec{\zeta},t)-u_{\theta,j}(\vec{\zeta},t)]+q_j(\vec{\zeta},t)\}\,\mathrm{d}A_j = \dot{M}[\langle h_{\mathrm{g,s}}\rangle - L_{\mathrm{eff}}] \tag{44}$$

where $\langle h_{\mathrm{g,s}}\rangle$ and L_{eff} are the averaged specific gas enthalpy at the liquid surface and the heat per unit mass for vaporization and interior heating of the droplet, respectively. L_{eff} is the sum of the latent heat of vaporization L and $(\dot{Q}_l/\dot{M})$ where $\dot{Q}_l$ is the heating rate of the droplet interior.

Now, we define

$$S_* \overset{\mathrm{def}}{=} \int_S \int G(\vec{x}-\vec{\zeta})\{p(\vec{\zeta},t)-\hat{p}(\vec{x},t)\}u_{\theta,j}(\vec{\zeta},t)\,\mathrm{d}A_j \tag{45}$$

Here, $u_{\theta,j}(\vec{\zeta},t)\,\mathrm{d}A_j$ is the rate of change of infinitesimal volume due to liquid–gas interface motion. After weighting with G and integrating over all liquid–gas interfaces in the volume, the negative of the time derivative of the void volume is obtained. So, if a droplet is locally in a spherically symmetric situation relative to the surrounding gas, this droplet's contribution to the S_* integral is proportional to the product of the pressure difference and the time derivative of the ratio of the droplet volume to the averaging volume. If there is only a Stefan velocity in the region and no imposed velocity, the gas velocity decreases with distance from the droplet and gas pressure increases with that distance. So, the differential surface pressure in the integral for S_* is negative. In this case, the S_* term represents differential pressure work done on the gas by the liquid which is changing volume. For vaporization (condensation), it is positive (negative) and acts as an energy source (sink) for the gas. The difference in pressure appears in the S_* term because of the definition of the average pressure given by Eq. (23).

For a translating particle with fore-and-aft symmetry in the surface-pressure distribution and without volume change or shape distortion, $S_* = 0$. If the flow separates over the translating particle, the integral for S_* is not equal to zero and work is done on the gas by the particle or on the particle by the gas. The fore-aft orientation and therefore the orientation of the net pressure drag force on the particle are determined by the vector $\langle u_i\rangle - \bar{u}_{l,i}$ and not by $\bar{u}_{l,i}$ alone. So, if the dot product $\bar{u}_{l,i}(\langle u_i\rangle - \bar{u}_{l,i})$ is negative, the particle is moving in a direction opposed to the net force and a positive value appears for S_*. That means that the particle is doing work on the continuous fluid (gas). If the dot product is positive, the integral is negative and work is done on the particle. The order of magnitude of the S_* term here will be given by the combined pressure-drag force of all particles in the averaging volume times the average particle velocity divided by the averaging

volume. Interestingly, it is not the total drag that contributes to this work term; the friction acts parallel to the surface, so, unlike the pressure, it does no work as the infinitesimal element of surface area sweeps over an infinitesimal volume.

These simple understandings about the pressure work can guide the creation of a model for the evaluation of S_*. For example, we can add the two effects discussed above to yield

$$S_* = \frac{1}{4\bar{\rho}_s}\left\{\frac{\dot{m}}{4\pi R}\right\}^2 \frac{\mathrm{D}(\bar{\theta})^2}{\mathrm{D}t} - \frac{3(1-\bar{\theta})}{8\bar{\theta}R}\bar{\rho}C_{\mathrm{D}_p}|\langle u\rangle - \bar{u}_l|\bar{u}_{l,j}(\langle u_j\rangle - \bar{u}_{l,j}) \tag{46}$$

where $\dot{m}$ is the vaporization rate of an average droplet, R is the instantaneous droplet radius, the time derivative following the gas is $\mathrm{D}(\ )/\mathrm{D}t = \partial(\ )/\partial t + \tilde{u}_j\partial(\ )/\partial x_j$, and C_{D_p} is the coefficient of pressure drag for the droplet. It is only suggested here that this model is worthy of testing, it is not endorsed yet. The S_* term is the flux of a velocity-squared term so it should be of the order of Mach number squared times a thermal flux term such as the divergence of E_i; so, for low-speed subsonic flows, it can be negligible.

Now, the averaged gas-phase energy equation becomes

$$\begin{aligned}&\frac{\partial(\bar{\rho}\langle h\rangle)}{\partial t} + \frac{\partial(\bar{\rho}\langle u_j\rangle\langle h\rangle)}{\partial x_j} + \frac{\partial \bar{q}_j}{\partial x_j} - \bar{\theta}\left\{\frac{\partial \hat{p}}{\partial t} + \langle u_j\rangle\frac{\partial \hat{p}}{\partial x_j}\right\}\\ &\quad = \bar{\Phi} + \sum_{n=1}^{N}\bar{\rho}\langle\omega_n\rangle Q_n + \dot{M}[\langle h_{\mathrm{g,s}}\rangle - L_{\mathrm{eff}}] + S_* - \Delta + \frac{\partial(\bar{\rho}E_j)}{\partial x_j}\end{aligned} \tag{47}$$

where

$$\Delta \overset{\mathrm{def}}{=} \langle u_j\rangle\bar{\theta}\frac{\partial \hat{p}}{\partial x_j} - \overline{u_j\frac{\partial p}{\partial x_j}} \tag{48}$$

$$E_i \overset{\mathrm{def}}{=} \langle u_i\rangle\langle h\rangle - \langle u_i h\rangle \tag{49}$$

The last four terms in Eq. (47) have not been recognized for spray flows before. The last term has been used in the turbulence community.

The averaged gas-phase equation of state may be expressed as

$$\bar{\theta}\hat{p} = \bar{\rho}\langle RT\rangle = \bar{\rho}[\langle h\rangle - \langle e\rangle] \tag{50}$$

where e is the specific internal energy. Note that for a multi-component mixture $\tilde{h}$ and $\tilde{e}$ must eventually be related to the average temperature $\widetilde{T}$ and the average mass fractions $\widetilde{Y}_n$, presenting another closure challenge. If the energy equation is re-formulated using Eq. (8) so that $\langle e\rangle$ becomes the dependent variable instead of $\langle h\rangle$, it will be seen that the total pressure at the droplet surface is critical in determining pressure work associated with volume change of the phase. This, of course, is consistent with the First Law of Thermodynamics.

The gas-phase species continuity equations, momentum equation, and energy equation can individually be placed in non-conservative form by combination of Eqs. (34), (43), or (47) with Eq. (33).

Of course, the same physics would be represented by the two-step averaging process, if the subgrid models were of high fidelity in both the one-step and two-step approaches. However, fidelity

of the sub-grid modelling is the problem with the two-step approach. Also, the same final forms for the species conservation equations, momentum equation, and energy equation would not be obtained in a two-step averaging process. If the first step averaged over droplet scales only but neglected turbulent fluctuations of smaller scale in the sub-grid model, the same forms as Eqs. (34), (43) and (47) would result after this first step with the same formal definition of the new flux terms. However, there would be obviously be differences in the modelling of the flux terms if turbulent fluctuations were not considered until the second step. The second averaging over the turbulent scales would produce still more flux terms because of the non-linearities. It would clearly be difficult to model the interactions between the smaller turbulent eddies and the droplets if the droplet physics had already been averaged and modelled in the first step. The results of the two-step averaging would also be different in the reverse situation where the turbulent-scale averaging and modelling were performed first, followed by the droplet-scale averaging and modelling. So, the one-step averaging offers the opportunity to model the droplet-scale physics, the smaller-eddy physics, and their interactions together with fewer flux terms.

2.5. Averaged vorticity and entropy

We can divide the non-conservative form of the momentum equation by the average density and then take the curl to yield an evolution equation for the average vorticity Ω_i which is here the curl of the mass-weighted average velocity and not the volume-weighted average of ω_i, the curl of velocity. The relationship between the two averages is given by

$$\begin{aligned}\bar{\omega}_i &= \epsilon_{ijk}\overline{\frac{\partial u_j}{\partial x_k}} = \epsilon_{ijk}\frac{\partial \bar{u}_j}{\partial x_k} - \epsilon_{ijk}\int_S \int G(\vec{x}-\vec{\zeta})u_j(\vec{\zeta},t)\,\mathrm{d}A_k \\ &= \Omega_i + \epsilon_{ijk}\frac{\partial(\bar{u}_j - \langle u_j\rangle)}{\partial x_k} - \epsilon_{ijk}\int_S \int G(\vec{x}-\vec{\zeta})u_j(\vec{\zeta},t)\,\mathrm{d}A_k \end{aligned} \tag{51}$$

where the permutation symbol $\epsilon_{ijk} = 0$ if two or three indices are identical, $+1$ if the indices reflect an even permutation of 123, and -1 if the indices reflect an odd permutation of 123. Part of the distinction (between the curl of the average velocity and the average of the curl) disappears if the integral of the cross-product of the normal surface vector and the tangential velocity vector over the droplet surface is zero. For a solid particle with no slip at the surface and no rotation, the surface velocity is the velocity of the particle's mass center and its tangential component varies from zero to the particle velocity value. The contribution of that particle to the surface integral in Eq. (51) becomes zero. If the particle is rotating in addition to translating, the surface integration, for that particle alone, of the cross-product of that tangential velocity and the normal surface vector will have a non-zero contribution whose value is proportional to the angular velocity and to the ratio of the particle's volume to the averaging volume. For a liquid droplet with internal circulation and/or a distortion that is symmetric about an axis, the surface integration will produce a zero value.

As noted by Sirignano (1972), the droplet aerodynamic force term and the droplet momentum source term will produce or modify the average vorticity even in the case of barotropic flow, negligible shear forces (away from the droplet surfaces), and zero initial vorticity. Our modification

here indicates that Γ_{ij} will also affect average vorticity Ω_i. The resulting vorticity evolution equation will be

$$\frac{\partial \Omega_i}{\partial t} + \langle u_j \rangle \frac{\partial \Omega_i}{\partial x_j} = \Omega_j \frac{\partial \langle u_i \rangle}{\partial x_j} - \Omega_i \frac{\partial \langle u_j \rangle}{\partial x_j} - \epsilon_{ijk} \frac{\partial (\bar{\theta}/\bar{\rho})}{\partial x_k} \frac{\partial \hat{p}}{\partial x_j} + \epsilon_{ijk} \left\{ \frac{\bar{\theta}}{\bar{\rho}} \frac{\partial^2 \hat{\tau}_{jr}}{\partial x_k \partial x_r} + \frac{\partial (\bar{\theta}/\bar{\rho})}{\partial x_k} \frac{\partial \hat{\tau}_{jm}}{\partial x_m} \right\} - \epsilon_{ijk} \left\{ \frac{\partial F_j}{\partial x_k} + \dot{M} \left\{ \frac{\partial \langle u_j \rangle}{\partial x_k} - \frac{\partial \bar{u}_{l,j}}{\partial x_k} \right\} + \frac{\partial \dot{M}}{\partial x_k} \{ \langle u_j \rangle - \bar{u}_{l,j} \} \right\} + \epsilon_{ijk} \frac{\partial^2 (\bar{\rho} \Gamma_{jr})}{\partial x_k \partial x_r} \tag{52}$$

An alternative choice of a method that obtains $\bar{\omega}_i$ directly is to combine the primitive equations (1) and (4) to obtain a non-conservative form, divide the result by density, then take the curl term-by-term to yield an evolution equation for ω_i, and finally perform the volume averaging. Thereby, it would be necessary to evaluate more product terms; so, this author prefers the other route outlined above.

Sirignano (1972) also obtained an evolution equation for the average entropy by combining the momentum and energy equations, neglecting some terms of the order of the Mach number squared (as appropriate for the combustion instability application of that publication) and assuming the same value of specific heat for each species. It was shown that the droplet interactions (exchange of mass and energy between the phases) produce entropy even in the absence of chemical reaction, heat and mass diffusion, and viscosity. Now, we improve on the accuracy of that relationship by averaging Eq. (9), still neglecting any variation in the specific heats across the species. The inclusions of the new terms and the higher order (in Mach number) effects now cause the averaged entropy conservation equation to be

$$\frac{\partial (\bar{\rho} \langle s \rangle)}{\partial t} + \frac{\partial (\bar{\rho} \langle u_j \rangle \langle s \rangle)}{\partial x_j} = \int_S \int G(\vec{x} - \vec{\zeta})(u_j - u_{0,j}) \rho s \, \mathrm{d}A_j + \frac{\partial (\bar{\rho} H_j)}{\partial x_j} + \frac{\overline{R}_1}{\widetilde{T}} + J \tag{53}$$

where based on the analysis of the averaged energy equation, we have

$$\overline{R}_1 = -\frac{\partial \bar{q}_j}{\partial x_j} + \overline{\Phi} + \sum_{n=1}^{N} \bar{\rho} \langle \omega_n \rangle Q_n - \dot{M} L_{\mathrm{eff}} \stackrel{\mathrm{def}}{=} R_2 - \dot{M} L_{\mathrm{eff}} \tag{54}$$

Furthermore, we define

$$H_i \stackrel{\mathrm{def}}{=} \langle u_i \rangle \langle s \rangle - \langle u_i s \rangle \tag{55}$$

and

$$J \stackrel{\mathrm{def}}{=} \overline{\left\{ \frac{R_1}{T} \right\}} - \frac{\overline{R}_1}{\langle T \rangle} \tag{56}$$

The integral in Eq. (53) reflects an entropy flux associated with mass transfer from the discrete phase. We can model that integral as $\dot{M} \langle s_{\mathrm{g,s}} \rangle$ where the subscripts imply the quantity is evaluated in the gas phase at the interface between the phases.

The averaged entropy conservation equation can be combined with the averaged continuity equation to obtain an averaged entropy-evolution equation.

$$\bar{\rho}\frac{\partial\langle s\rangle}{\partial t}+\bar{\rho}\langle u_j\rangle\frac{\partial\langle s\rangle}{\partial x_j}=\dot{M}\left(\langle s_{g,s}\rangle-\langle s\rangle-\frac{L_{\text{eff}}}{\langle T\rangle}\right)+\frac{\partial(\bar{\rho}H_j)}{\partial x_j}+\frac{R_2}{\langle T\rangle}+J \tag{57}$$

A reasonable model for the averaged entropy difference is

$$\langle s_{g,s}\rangle-\langle s\rangle-\frac{L_{\text{eff}}}{\langle T\rangle}=\frac{\langle h_{g,s}\rangle-\langle h\rangle-L_{\text{eff}}}{\langle T\rangle} \tag{58}$$

Clearly, now the effect of mass and energy exchanges between the phases as indicated by $\dot{M}[\langle h_{g,s}\rangle-\langle h\rangle-L_{\text{eff}}]$ is seen to affect entropy production.

2.6. Averaged liquid-phase partial differential equations

The averaged equations for the liquid phase can be developed by multiplying every term in Eqs. (1)–(7) by the product of G and $(1-\theta)$. For the constant-density liquid, mass weighting and volume weighting produce the same average. First, we obtain the averaged liquid-phase continuity equation

$$\frac{\partial\bar{\rho}_l}{\partial t}+\frac{\partial(\bar{\rho}_l\bar{u}_{l,j})}{\partial x_j}=-\dot{M} \tag{59}$$

Next, the averaged liquid-phase species continuity equation can be written. The Gauss divergence theorem will show that there will be a contribution to the divergence of $\overline{\rho_l Y_{l,n}V_{l,n,i}}$ coming only from the portions of the boundary of the averaging volume that intersect the volumes of droplets located on the boundary. A large Peclet number can be considered, liquid-phase mass diffusion is slow compared to advection of the liquid-phase species across the averaging-volume boundaries. Therefore, we can neglect this diffusion contribution compared to other terms for spray applications. (Liquid-phase mass diffusion might be important, however, for some other multi-phase application.) The average diffusion flux goes to zero. So, it can be shown that

$$\overline{\rho_l Y_{l,n}V}_{l,n,i}=\bar{\rho}_l\overline{Y_{l,n}V}_{l,n,i}=\bar{\rho}_l\overline{Y}_{l,n}\overline{V}_{l,n,i}-\bar{\rho}_l\bar{\beta}_{l,n,i}=0 \tag{60}$$

It follows that

$$\frac{\partial(\bar{\rho}_l\overline{Y}_{l,n})}{\partial t}+\frac{\partial(\bar{\rho}_l\overline{Y}_{l,n}\bar{u}_{l,j})}{\partial x_j}=-\dot{M}\epsilon_{l,n}+\frac{\partial(\bar{\rho}_l\alpha_{l,n,j})}{\partial x_j},\quad n=1,\ldots,N \tag{61}$$

The averaged liquid-phase momentum equation for the vaporizing case is

$$\frac{\partial(\bar{\rho}_l\bar{u}_{l,i})}{\partial t}+\frac{\partial(\bar{\rho}_l\bar{u}_{l,i}\bar{u}_{l,j})}{\partial x_j}+(1-\bar{\theta})\frac{\partial\hat{p}_l}{\partial x_i}=(1-\bar{\theta})\frac{\partial\hat{\tau}_{l,ij}}{\partial x_j}+\bar{\rho}_l g_i+F_i-\dot{M}\bar{u}_{l,i}+\frac{\partial(\bar{\rho}_l\Gamma_{l,ij})}{\partial x_j} \tag{62}$$

Note that the next-to-last term in Eq. (62) must be modified to read $\dot{M}\langle u_i\rangle$ for the case of condensation. This momentum equation can be developed further by making a standard assumption that the gradient of the averaged pressure and the gradient of the averaged viscous stress tensor at any point $\vec{x}$ are identical for the two phases. Note that capillary effects can prevent the matching of pressure and viscous stress across the gas/liquid interface. Capillary pressure causes a jump in pressure across the interface, however, for spherical droplets, that jump quantity is uniform along the interface; so, the pressure gradients on the two sides match. If surface temperature and/or sur-

face composition varies along the surface, viscous stress can jump across the interface and the pressure jump can become non-uniform along the surface. However, if the droplet interior field is axisymmetric, these effects average to zero effect on the gradients. Solving for these gradients from Eq. (43) and substituting into Eq. (62), we find

$$\frac{\partial(\bar{\rho}_l\bar{u}_{l,i})}{\partial t}+\frac{\partial(\bar{\rho}_l\bar{u}_{l,i}\bar{u}_{l,j})}{\partial x_j}=\frac{1-\bar{\theta}}{\bar{\theta}}\bar{\rho}\frac{\mathrm{D}\langle u_i\rangle}{\mathrm{D}t}+\left\{\bar{\rho}_l-\bar{\rho}\frac{1-\bar{\theta}}{\bar{\theta}}\right\}g_i+\frac{F_i}{\bar{\theta}}-\dot{M}\left\{\frac{\bar{u}_{l,i}}{\bar{\theta}}-\frac{1-\bar{\theta}}{\bar{\theta}}\langle u_i\rangle\right\}+\frac{\partial(\bar{\rho}_l\Gamma_{l,ij})}{\partial x_j}-\frac{1-\bar{\theta}}{\bar{\theta}}\frac{\partial(\bar{\rho}\Gamma_{ij})}{\partial x_j} \tag{63}$$

For the liquid-phase energy equation, we can again use the Gauss divergence theorem to show that there will be a contribution to the divergence of $\bar{q}_{l,i}$ coming only from the portions of the boundary of the averaging volume that intersect the volumes of droplets located on the boundary. We can consider this contribution to be negligible compared to other terms for spray applications. This could be important, however, for some other multi-phase application. The averaged liquid-phase energy equation can now be written as

$$\frac{\partial(\bar{\rho}_l\bar{h}_l)}{\partial t}+\frac{\partial(\bar{\rho}_l\bar{h}_l\bar{u}_{l,j})}{\partial x_j}=(1-\bar{\theta})\left\{\frac{\partial\bar{p}_l}{\partial t}+\bar{u}_{l,j}\frac{\partial\bar{p}_l}{\partial x_j}\right\}+\overline{\Phi}_l-S_{l,*}-\Delta_l-\dot{M}[\langle h_{\mathrm{g,s}}\rangle-L_{\mathrm{eff}}]+\frac{\partial(\bar{\rho}_lE_{l,j})}{\partial x_j} \tag{64}$$

Again, the last term in Eq. (61), the last term in Eq. (62), and the last three terms in Eq. (64) have not been recognized for two-phase flows before. The equations are constructed so that energy flux into the droplet surface from the gas (or work done by the gas on the droplet surface) does not necessarily equal in magnitude the energy flux into the liquid (or work done on the liquid) because capillary action causes a pressure jump across the interface and surface energy can change as the droplet size, shape, temperature, and/or composition change. $S_{l,*}$ is determined by a modified form of Eq. (45) with the surface pressure defined on the liquid side of the interface and the average pressure is the average for the liquid phase. Due to the capillary actions, these liquid-pressure values will be higher than the corresponding gas-pressure values indicated in that equation. So, while a positive S_* represents work (per unit volume per unit time) done on the gas by the differential pressure at the gas side of the interface as the liquid volume changes, it is not generally equal to the value of $S_{l,*}$ which represents work done by the differential pressure force on the liquid side of the interface. The difference is caused by the integral of the product of interface velocity $u_{\theta,j}$ and the difference between the local capillary pressure at the surface and the average capillary pressure. In the special case of spherical droplets, $u_{\theta,j}$ and the capillary pressures are uniform in magnitudes over the interface with the average and local capillary pressures equal, so, the difference between S_* and $S_{l,*}$ disappears.

2.7. Averaged liquid-phase Lagrangian equations

In developing the Lagrangian form of the equations, we define the time derivative following the liquid $\mathrm{d}(\ )/\mathrm{d}t=\partial(\ )/\partial t+\bar{u}_{l,j}\partial(\ )/\partial x_j$. The liquid density is considered to be constant so that $\bar{\rho}_l=[1-\bar{\theta}]\rho_l$.

Recognizing that, for constant liquid density, $\bar{\rho}_l = \rho_l[1-\bar{\theta}] = n\rho_l V_{\text{drop}}$ where $n(\vec{x},t)$ is the droplet number density and $V_{\text{drop}}(\vec{x},t)$ is the average droplet volume, we may construct two other equivalent forms of the liquid-phase continuity equation:

$$\frac{\mathrm{d}\bar{\theta}}{\mathrm{d}t} = -\frac{\partial(1-\bar{\theta})}{\partial t} + \frac{\partial((1-\bar{\theta})\bar{u}_{l,j})}{\partial x_j} = \frac{\dot{M}}{\rho_l} \tag{65}$$

or

$$\frac{\mathrm{d}V_{\text{drop}}}{\mathrm{d}t} = \frac{\partial V_{\text{drop}}}{\partial t} + \bar{u}_{l,j}\frac{\partial V_{\text{drop}}}{\partial x_j} = -\frac{\dot{M}}{\rho_l n} = -\frac{\dot{m}}{\rho_l} \tag{66}$$

where $\dot{m}(\vec{x},t)$ is the mass vaporization rate of an average droplet. In the last equation, it has been assumed that the total number of droplets is conserved, i.e., there is no coalescence or shattering and $\partial n/\partial t + \partial(n\bar{u}_{l,j})/\partial x_j = 0$.

Eqs. (34), (62) and (64) can be reorganized into non-conservative and Lagrangian forms. The species continuity equation becomes

$$\bar{\rho}_l\frac{\mathrm{d}\overline{Y}_{l,n}}{\mathrm{d}t} = \bar{\rho}_l\frac{\partial\overline{Y}_{l,n}}{\partial t} + \bar{\rho}_l\bar{u}_{l,j}\frac{\partial\overline{Y}_{l,n}}{\partial x_j} = -\dot{M}[\epsilon_{l,n} - \overline{Y}_{l,n}] + \frac{\partial(\bar{\rho}_l\alpha_{l,n,j})}{\partial x_j}, \quad n = 1,\ldots,N \tag{67}$$

The averaged liquid-phase momentum equation in non-conservative and Lagrangian forms becomes

$$\begin{aligned}\bar{\rho}_l\frac{\mathrm{d}\bar{u}_{l,i}}{\mathrm{d}t} &= \bar{\rho}_l\frac{\partial\bar{u}_{l,i}}{\partial t} + \bar{\rho}_l\bar{u}_{l,j}\frac{\partial\bar{u}_{l,i}}{\partial x_j}\\ &= \frac{1-\bar{\theta}}{\bar{\theta}}\bar{\rho}\frac{\mathrm{D}\langle u_i\rangle}{\mathrm{D}t} + \left\{\bar{\rho}_l - \bar{\rho}\frac{1-\bar{\theta}}{\bar{\theta}}\right\}g_i + \frac{F_i}{\bar{\theta}} - \dot{M}[\langle u_i\rangle - \bar{u}_{l,i}]\frac{1-\bar{\theta}}{\bar{\theta}} + \frac{\partial(\bar{\rho}_l\Gamma_{l,ij})}{\partial x_j}\\ &\quad - \frac{1-\bar{\theta}}{\bar{\theta}}\frac{\partial(\bar{\rho}\Gamma_{ij})}{\partial x_j}\end{aligned} \tag{68}$$

The averaged liquid-phase energy equation in non-conservative or Lagrangian form is

$$\begin{aligned}\bar{\rho}_l\frac{\mathrm{d}\bar{h}_l}{\mathrm{d}t} - (1-\bar{\theta})\frac{\mathrm{d}\hat{p}_l}{\mathrm{d}t} &= \bar{\rho}_l\frac{\partial\bar{h}_l}{\partial t} + \bar{\rho}_l\bar{u}_{l,j}\frac{\partial\bar{h}_l}{\partial x_j} - (1-\bar{\theta})\left\{\frac{\partial\hat{p}_l}{\partial t} + \bar{u}_{l,j}\frac{\partial\hat{p}_l}{\partial x_j}\right\}\\ &= \overline{\Phi}_l + \dot{Q}_l - S_{l,*} - \Delta_l + \frac{\partial(\bar{\rho}_l E_{l,j})}{\partial x_j}\end{aligned} \tag{69}$$

The following relationships have been used: $L_{\text{eff}} = L + \dot{Q}_l/\dot{M} = \langle h_{\text{g,s}}\rangle - \bar{h}_l + \dot{Q}_l/\dot{M}$.

There is somewhat of a misnomer in describing this system as a Lagrangian system of equations. Normally in a Lagrangian tracking, we follow a fixed element of mass. (This in contrast to an Eulerian calculation where we deal with a fixed volume.) The Lagrangian element normally can change its volume and shape, changes of phase and chemistry can occur, and exchanges of equal amounts of mass can occur with its environment can occur, but it remains the amount of same mass. However, in the system of equations here, the averaging volume at each instant of Lagrangian time will have the same magnitude and shape but the amount of mass in this volume can change. It is better therefore in mathematical terms to describe this as a method

of characteristics (Sirignano, 1999). Note that one could create a truly Lagrangian system for the liquid-phase equations by making the vectors $\vec{x}$, $\vec{\xi}$, and $\vec{\zeta}$ in the averaging integration reflect initial positions (rather than instantaneous positions) and thereby always identify the same points of mass. The problem would come then with the match with the gas-phase equations, namely, the averagings would not occur over the same field. So, in a true Lagrangian formulation, it would be very difficult to sensibly describe exchanges of mass, momentum, and energy between the phases. So, we remain with the pseudo-Lagrangian scheme that locally and instantaneously uses a fixed volume for the averaging integration.

The number of droplets in the averaging volume can change in accordance with the droplet number conservation equation. Written in Lagrangian form, that equation becomes

$$\frac{\mathrm{d}n}{\mathrm{d}t} = -n\frac{\partial \bar{u}_{l,j}}{\partial x_j} \tag{70}$$

So, one approach to the calculations is to determine the varying droplet number density using Eq. (70) and to relate $\dot{M}$ to $\dot{m}$ through the use of n as indicated by Eq. (66). Another approach, that will also conserve droplet numbers, is to fix the number of droplets associated with each characteristic path at the value given by an initial condition or inflow boundary condition.

An alternative analysis of the liquid properties could be developed following an approach presented by Sirignano (1999). The droplets could be separated into N^* different classes based upon their initial properties, e.g., diameter, velocity, or point of injection. A set of conservation equations (or evolution equations) could be developed for each droplet class. We will not provide the details here.

It must be understood that the problem of a spray with rapidly vaporizing droplets in a high-temperature gaseous environment requires more knowledge of the microstructure than is provided by the above averaged liquid-phase equations. For example, the temporal and spatial variations of temperature and composition in the liquid droplet must be resolved via modelling (Sirignano, 1999) for accurate prediction of heat and mass exchange between the phases. The internal fluid motion of the droplet can affect the transport and must also be resolved by modelling. These models can be used to predict liquid temperature and composition in place of Eqs. (61) and (64) or equivalently (67) and (69).

3. Importance of the various flux terms

3.1. Laminar microstructures

Let us now analyze the contribution of the gas-phase flux terms $\alpha_{n,i}$, $\beta_{n,i}$, Γ_{ij}, Δ, and E_i. The results will depend on the microstructure of the flow within the averaging volume. The flux terms will also depend on the magnitude of the averaging volume and, through these terms and a few other source terms in the equations, the size of the averaging volume will affect the averaged quantities governed by the equations: e.g., ρ, u_i, Y_n, and h. In spectral terms, the larger the averaging volume is, the larger is the minimum wavelength left unfiltered by the averaging. These terms are known to be important in LES calculations where the averaging volume is larger than the smallest turbulent eddies. We will focus at first here on cases where the smallest vortical eddies are larger

than the averaging volume, so the microstructure is laminar. In the next subsection, we shall discuss the case where some eddies are smaller than the volume.

Some of these flux terms have been reported in the literature on two-phase flows and porous-media flows. Zhang and Prosperetti (1994a,b) used multi-realization averages to treat disperse flows without mass exchange between phases, viscosity, heat transfer, or compressibility. They considered potential flow in the microstructure and used an expansion with $1-\bar{\theta}$ as the perturbation parameter. The present analysis is different in that we consider the continuous fluid and the disperse fluid to be multi-component, account for viscosity, heat transfer, and chemical reaction, and allow the continuous flow density to vary due to compression (or expansion) and/or heating (or cooling). Also, the perturbation expansion is not useful here because although the gas volume is orders of magnitude larger than the liquid volume, the mass, momentum, and energy of the discrete liquid phase are of the same order of magnitude or not more than one order less than the counterpart continuous gas properties. In a later paper, Zhang and Prosperetti (1997) added the effects of heat conduction and viscosity but still did not allow compressibility, mass exchange, chemical reaction, or multi-component character. They also advocate the use of particle equations for the discrete phase which track global characteristics of the particles without requiring resolution of the microstructure of the discrete-fluid field. As noted earlier, these particle equations might "wash away" interesting physics for certain problems, e.g., rapidly vaporizing droplets.

Early papers (Whitaker, 1966, 1967; Slattery, 1967) on flows through porous media employed volume averaging to develop equations governing the hydrodynamics (e.g., Darcy's law). Whitaker (1967) discusses the dispersion vector α_i for a single, non-adsorbing, non-reacting species in an incompressible porous flow. Later, Whitaker (1973) extended the transport equations to consider multi-component diffusion, chemical reaction, and change of phase, the paper focused on mass transfer and did not consider the coupling with the equations for momentum and energy conservation. So, in addition to unifying the averaging methods for two-phase flows, LES analyses, and practical computation, the current work does extend and strengthen the theoretical foundations for two-phase flows.

The purpose here will not be to develop a general model for the microstructure but rather to examine where these flux terms might have quantitative importance. So, we study here only a few very simple descriptions of droplet arrays undergoing heat, momentum, and mass exchanges with the gas. These model problems are intended to reflect the most essential physics and to help determine roughly the magnitudes of these flux terms. They need not be the basis of further modelling of these terms but can help to determine whether further consideration of these terms should occur.

Let us consider a combustion application where liquid mass of fuel is injected at roughly stoichiometric proportions into air at a pressure of O(10 atmospheres). Assume that droplet diameters initially are in the range of 10–100 μm. Since the ratios of liquid density to air density and of total air mass to total liquid mass are of O(100) and O(10), respectively, we can estimate that the ratio of total initial liquid volume (before substantial vaporization has occurred) to total gas volume is O(1000). Then, the average spacing between neighboring droplets is O(10 diameters) or 100 μm to 1 mm. Three-dimensional computational fields are typically divided into $O(10^5)$ to $O(10^7)$ computational cells. In a typical computation for a combustor that might have a characteristic length of 10 cm to a meter, the computational cell would therefore have a corresponding

dimension of 1 mm to a centimeter. So, a computational cell could have from O(1) to O(10^6) droplets within it. As noted earlier, in order to optimize resolution, the averaging volume should have the same order of magnitude as the computational cell volume. Clearly, at the lower end of this range, a statistical sample of droplets will not exist in the volume over which the averaging occurs. So, with only a few droplets in the volume, the averaged results become more sensitive to variations in specific locations and velocities of the droplets. With at least O(10–100) droplets in the volume, we can have more confidence in our predictive capability for any specific realization. So, in some cases, it might be desirable not to minimize the computational cell volume to the full extent allowed by available computational resources. Rather, the cell volume could be chosen to contain a sufficient number of droplets, then the smaller-scale physics could be modelled. Through the use of reasonable models for droplet behavior (Sirignano, 1999) and sub-grid turbulent fluctuations (Piomelli, 1999; Givi, 2003), the description of the physics can be extended to length scales below those of the averaging volume and computational cell.

For simplicity, Fourier heat conduction, Fickian mass diffusion, and Newtonian viscosity will be considered with the Prandtl number and Schmidt number to each have unity value. Note that the particular fluxes under consideration are invariant under a Galilean transformation, so we will use a reference frame moving with the cloud of droplets locally (all droplets in the averaging volume have the same velocity in this exercise) so that there is a steady or at least quasi-steady situation. We will examine two general cases: one case with a cloud of vaporizing droplets without forced or natural convection but only Stefan convection and another case with relative motion between the droplets in a cloud and the ambient gas.

In the first case with only Stefan convection, the product of gas density and velocity will be the gradient of a potential function. It has been shown in several papers on arrays of vaporizing droplets that the governing diffusive–advective equation can be transformed to Laplace's equation, the scalar quantity is an exponential function of the potential, and therefore the gradient of the scalar is aligned locally to be parallel with the Stefan velocity (see Labowsky, 1980; Umemura et al., 1981a,b; Imaoka and Sirignano, 2003, 2004). If the distribution of droplets with regard to size and location is symmetrical over the averaging volume, the average Stefan velocity u_i in the volume will be zero and the average of the scalar-velocity product will be zero since each droplet acts as a monopole source for mass and as a monopole sink for heat. The same result occurs with the diffusion velocity $V_{n,i}$. So, $\alpha_{n,i}$, $\beta_{n,i}$, and E_i would each be zero. However, asymmetrical droplet distribution over a finite averaging volume will make those averages different from zero. See, for example, the simple asymmetrical situation sketched in Fig. 1. The magnitudes of these fluxes remains to be determined but it is seen that, with significant asymmetry of the droplet distribution, the scalar fluxes could become of the order of the product of the average scalar and the average velocity. In that situation, the flux term can have importance.

Recent calculations (Imaoka and Sirignano, 2003, 2004) indicate that for two droplets (with only Stefan convection) placed asymmetrically within a rectangular control volume, the $\alpha_{n,i}$ and E_i flux terms will be less than 10% of the largest flux terms in the equation. The term Γ_{ij} can be significant for symmetric or asymmetric microstructural configurations. The quantity $u_i u_j$ is everywhere positive for $i = j$ and thereby $\overline{u_i u_j} > 0$. For a symmetric case, $\bar{u}_i = 0$, so, clearly Γ_{ij} can be significant in the momentum equation, i.e., Eq. (43).

In the second problem as portrayed in Fig. 2, we examine the wakes of an array of vaporizing droplets. The linearized approach for slender axisymmetric far wakes described in many texts (see

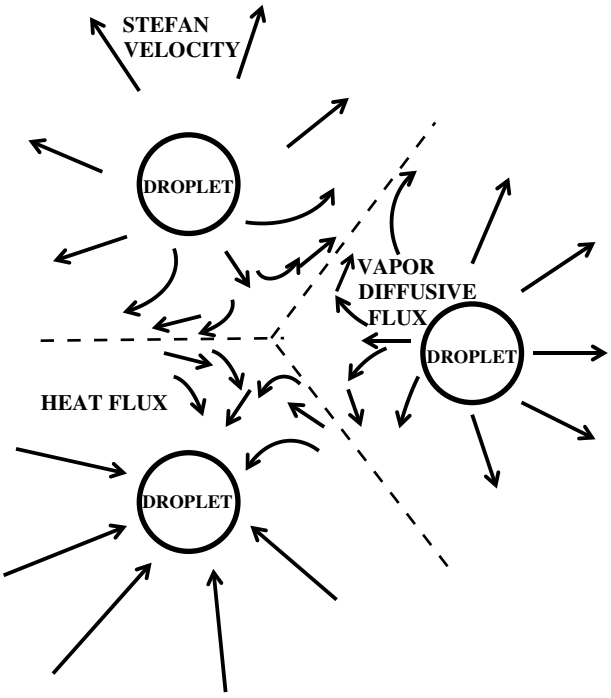

Fig. 1. Vaporizing droplet-array with Stefan flow.

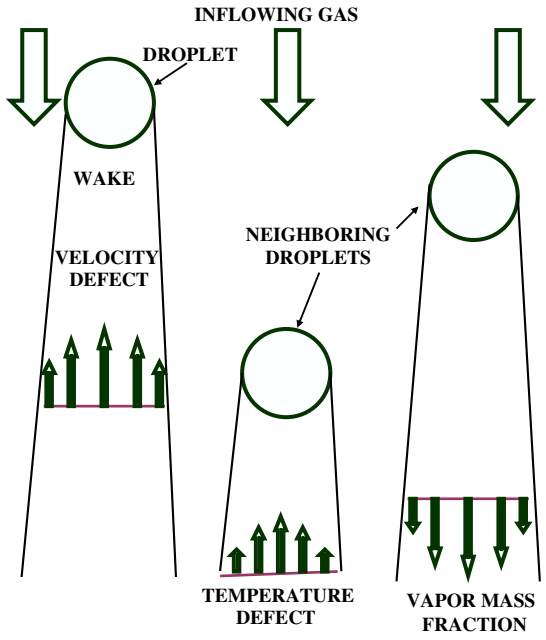

Fig. 2. Vaporizing droplet-array wake flows.

for example White, 1991) will be followed. The analysis is presented in Appendix A. The magnitude of Γ_{11} is found to be roughly a factor of $O(10^{-2})$ to $O(10^{-1})$ times the square of the average velocity component in the range $10 < Re < 100$. Therefore, it might be sufficiently important to consider as a correction for laminar two-phase flows. For typical fuels and the conditions considered here, $E_1/(\bar{u}\bar{h})$ is possibly an $O(10^{-1})$ quantity and $\alpha_{F,1}/(\bar{u}\bar{h})$ is an $O(10^{-1})$ or higher quantity. So, they can be important corrections. More attention must be paid to the microstructure behavior in order to have good predictions on a larger scale.

The Δ term depends on the pressure gradient. So, if that pressure gradient is balanced primarily by the inertial term (spatial acceleration), it will differ from the thermal energy flux term such as the divergence of E_i by a factor of the order of the square of the flow Mach number. If the pressure gradient is balanced primarily by the local acceleration term in unsteady cases or by the viscous stress term, we can expect the factor to be of the order of the Mach number. So, for the wide range of cases where the flow in the microstructure is at low subsonic speeds, the Δ term should be insignificant compared to other terms.

Each of these same flux terms discussed here for the gas phase has a counterpart in the liquid phase. The discrete phase for sprays has the advantage that it is less difficult to model than the gas phase. Models for heat and mass transport and internal fluid motion within droplets do exist in the literature (see for example Sirignano, 1999). So, models for the five averaged flux terms could be developed with some reasonable effort and would be an interesting future exercise. However, because decent microscale models exist for the internal liquid behavior, another route for calculations has been followed. The internal velocity, temperature, and composition have been spatially and temporally resolved by means that are not excessively computationally intensive. As a result, Eqs. (61) and (64) or equivalently (67) and (69) can be bypassed. Instead, the models provide the spatially resolved solutions for an average droplet, including, the properties on the droplet surface. Still, in order to determine the trajectories of these average droplets, Eq. (63) or (68) must be solved simultaneously with the equations of the model.

3.2. Vortex–droplet interactions

Sirignano (1972) predicted that the droplet (or particle) aerodynamic forces and the momentum exchange associated with mass exchange (e.g., vaporization) caused the production of vorticity in a two-phase flow. This occurs independently of whether or not unsteady boundary layers or wakes are developed around the droplets. The existing DNS research clearly indicates that the presence of particles or droplets affects the high wave number (small turbulent scale) end of the energy spectrum. Therefore, the dissipation of turbulent kinetic energy can also be affected. There is also evidence that the turbulence–particle interactions can create a less homogeneous situation on the level of the microstructure. That is, an initially uniform distribution of particles (in terms of interparticle spacing) can be made highly non-uniform by the turbulence. These findings indicate that there is good reason to pursue examination of the situation where the smallest turbulent scales can be comparable to the droplet or particle scales. Also, the role of stratification within the microstructure is worthy of further examination.

The evaluation in the previous subsection considered a laminar flow on the scale of the microstructure. That is, any vortex structures were larger than the averaging volume. Now, we consider briefly situations where the smallest vortex structure are on the scale of the droplet diameter or

spacing. There has been some research on the interactions of small vortex structures with particles and droplets based on the solutions of the Navier–Stokes equations (see Kim et al., 1995, 1997; Masoudi and Sirignano, 1997, 1998, 2000). The indications are that significant modifications of mass, momentum, and heat exchange can occur when a vortex collides with a particle or droplet. The existing models for droplet drag, heating rate, and vaporization rate are built for laminar microstructures and are inaccurate here. Kim et al. (1995, 1997) found that significant modifications in the droplet drag can occur due to the unsteady vortex/droplet interaction. They also showed that the interaction between vortices and droplets causes the creation of lift and torque on the droplet. Masoudi and Sirignano (2000) demonstrated significant modifications of the Sherwood number for a vaporizing droplet via interactions with vortices. The average vaporization rate can be increased or decreased by a 10% or more factor. The algebraic sign of the modification depends on the geometric relationship between the droplet and vortex (or vortices) and the direction of vortical rotation. Masoudi and Sirignano (1998) showed that vortex–solid particle interactions can have especially significant modification of the Nusselt number when the gas temperature is spatially non-uniform. So, it can be strongly suspected that, for a vaporizing droplet, the non-uniform vapor concentration in the gas surrounding a droplet in synergism with a vortex (or vortices) will substantially increase the magnitude of the difference between vaporization rate for axisymmetric droplet situations and the rate for a droplet interacting with a vortex (or vortices). The works of Kim et al. and Masoudi and Sirignano provide various correlations for aerodynamic coefficients and Nusselt and Sherwood numbers that can be applied as a first approximation for sub-grid modelling to describe droplet interactions with the smallest vortices. A correlation, for example, is given between Sherwood number and a function of vortex circulation strength, droplet Reynolds number, and distance between droplet and vortex trajectories. The correlations apply to only specific configurations, however. In summary therefore, new models for a wider range of configurations are definitely needed to predict the droplet aerodynamic force F_i and the vaporization rate $\dot{m}$ for two-phase LES calculations where vortices are sized at the magnitude of the droplet scale.

The gas-phase flux terms $\alpha_{n,i}$, $\beta_{n,i}$, Γ_{ij}, and E_i are well known to be important in single-phase LES calculations. Models of these terms can be found in the literature. Here, we have shown the importance of these terms for two-phase laminar or turbulent flows. There is good reason to assume that the proper flux models for two-phase, turbulent microstructure should be different from models that apply to single-phase turbulent flows or from models for laminar two-phase flows. It is expected that the model for viscous dissipation Φ will differ for two-phase flows since Ferrante and Elghobashi (2003) and others have shown that the high wavenumber end of the energy spectrum is affected by the presence of particles. As noted above, several researchers have found that, contrary to intuition about mixing, turbulence can make the distribution of inter-droplet spacing highly non-uniform. This can increase the degree of spacial variation of the properties within the microstructure and cause terms related to the differences between averages of products and products of averages to be quite significant quantitatively.

4. Concluding remarks

The volume-averaging process for spray flows has been formulated and evaluated. While the motivation for this analysis has been spray flows, the theoretical foundations apply to a very wide

range of laminar and turbulent multi-phase systems where the microstructure cannot be fully resolved and averaging is required. The optimization of the relationship between the volume used in the averaging process and the volume associated with numerical discretization of the partial differential equations has been discussed. Averaging methodology for LES and for two-phase flow have been unified at the most fundamental level; this is a unique aspect of this approach which avoids two sequential averaging processes. The value of the consistency between volumes over which averages are made and computational-cell volumes have been noted. Furthermore, the complicating effects of spatial variation of the size, shape, and/or orientation of the averaging volume has been shown. However, substantially more work on microstructure (sub-grid) modelling is required. Evidence has been provided for the importance of the flux terms $\alpha_{n,i}$, $\beta_{n,i}$, Γ_{ij}, and E_i in the equations governing the spray flow. The need for further attention to the modelling of those terms has been indicated. In particular, the situation must be further analyzed where the smallest turbulent scales are of the same order or smaller than the average distance between neighboring droplets; the significance of the effects of droplet collisions with small vortices on the exchange rates for mass, momentum, and energy have been indicated. The pressure work terms $S_{l,*}$ and S_* have been identified and explained. The averaged partial differential equations for the gas-phase properties and for the liquid-phase properties in a vaporizing, multi-component, reacting gas flow has been formulated with several new flux terms and a new work term. Evolution equations for averaged entropy and averaged vorticity have been advanced. The difference between the curl of the average velocity and the average of the velocity curl has been identified and related to the rotation of the discrete particles or droplets. The liquid-phase equations have also been presented in a "Lagrangian" form and some subtleties about the implications of that form have been discussed.

Appendix A. Droplet wake analysis

Each droplet in an array within the averaging volume has a wake; it is considered that droplet spacing is sufficient to neglect the interaction of any wake with another wake or droplet. The microstructure here is analyzed using the primitive equations first and then averaging the results. The common free-stream velocity is U_0 in a frame of reference moving with the droplet and the Reynolds number (Re) value is appropriate for laminar boundary layer to apply. For velocity defect $u_1 = U_0 - u \ll U_0$, where u is the actual velocity after the Galilean transformation, a linear theory (White, 1991) yields the result

$$\frac{u_1}{U_0} = \frac{C_D\, Re}{8x/R} \exp\left\{-\frac{U_0 r^2}{4\nu x}\right\} \tag{A.1}$$

where r, x, R, C_D, and ν are the streamwise coordinate, the radial coordinate in the cylindrical scheme, the droplet radius, the droplet drag coefficient, and the kinematic viscosity, respectively. We neglect here, within the first approximation, momentum exchange between the droplet and gas due to mass exchange. Under the assumptions that specific heat c_p is constant, Schmidt number $Sc = 1$ and Prandtl number $Pr = 1$, we have for the temperature defect T_1 and the fuel vapor mass fraction Y_F that

$$\frac{T_1}{T_0} = \frac{\dot{m} L_{\text{eff}}}{4\pi\rho c_p T_0 \nu x} \exp\left\{-\frac{U_0 r^2}{4\nu x}\right\} \tag{A.2}$$

and

$$Y_{\text{F}} = \frac{\dot{m}}{4\pi\rho\nu x} \exp\left\{-\frac{U_0 r^2}{4\nu x}\right\} \tag{A.3}$$

where the pre-exponential terms are determined by integrating the profile over the cross-sectional area to obtain the total energy (or species mass) flux and matching to the energy (or mass) exchange rate with the droplet.

The results from the linear theory for each droplet can be summed to give the results for a droplet array, including the effects of some overlap of the expanding wakes. With $C_{\text{D}} Re = \text{O}(10)$, the wake will extend downstream about 100 droplet diameters or about 10 droplet spacings. The common free stream velocity for droplets in the array assures that the axisymmetric wake centerlines for the various droplets are parallel. So, the average lateral spacing between wake centerlines for adjacent wakes is $\text{O}(10^{1/2})$ droplet diameters. This means that the cross-sectional area A of air flow "assigned" to each droplet is about 10 square diameters. The e-folding radius of the widening wake given by Eq. (A.1) at 100 diameters downstream is about 1.4 droplet diameters at $Re = 100$ and about 4.5 diameters at $Re = 10$. The probability of one droplet to be centered in the wake of another droplet is sufficiently small that we will neglect it.

Now, we seek the average values over the volume. For this linearized problem, the first approximation uses a uniform density so that there is no difference between a volume-weighted average and a mass-weighted average. Note that the integrations of Eqs. (A.1)–(A.3) over a cross-section orthogonal to the flow direction x give results that are independent of x. So, it immediately gives the volume average as well as the cross-sectional average following division by the cross-sectional area. The average quantities and the perturbations from the averages are

$$\begin{aligned} \bar{u} &= U_0\left\{1 - \frac{\pi R^2}{A}\frac{C_{\text{D}}}{2}\right\} \\ u'(x,r) &= u - \bar{u} = U_0\left\{\frac{\pi R^2}{A}\frac{C_{\text{D}}}{2} - \frac{C_{\text{D}} Re}{8x/R}\exp\left\{-\frac{U_0 r^2}{4\nu x}\right\}\right\} \end{aligned} \tag{A.4}$$

$$\begin{aligned} \overline{T} &= T_0\left\{1 - \frac{\dot{m} L_{\text{eff}}}{\rho U_0 A c_p T_0}\right\} \\ T'(x,r) &= T - \overline{T} = \frac{\dot{m} L_{\text{eff}}}{\rho U_0 A c_p}\left\{1 - \frac{A}{\pi R^2}\frac{Re}{4x/R}\exp\left\{-\frac{U_0 r^2}{4\nu x}\right\}\right\} \end{aligned} \tag{A.5}$$

and

$$\begin{aligned} \overline{Y}_{\text{F}} &= \frac{\dot{m}}{\rho U_0 A} \\ Y'_{\text{F}} &= \frac{\dot{m}}{\rho U_0 A}\left\{\frac{A}{\pi R^2}\frac{Re}{4x/R}\exp\left\{-\frac{U_0 r^2}{4\nu x}\right\} - 1\right\} \end{aligned} \tag{A.6}$$

Note that with the given spacing the quantity $\pi R^2/A$ is $O(10^{-1})$. Neglecting terms of $O((\pi R^2/A)^2)$, we can show that

$$\frac{\Gamma_{11}}{\bar{u}\bar{u}} = -\frac{\overline{u'u'}}{U_0 U_0} = -\frac{C_D^2}{32}\frac{\pi R^2}{A} Re \frac{\log(L/R)}{L/R} \tag{A.7}$$

where L is the wake length over which integration has occurred. $x/R = O(1)$ is the approximate length to the point where the velocity deficit is of $O(U_0)$; we begin our integration there. We normalize the quantity so that the average of the product can easily be compared to the product of the averages. The normalized Γ_{11} is estimated to be roughly between $O(10^{-2})$ and $O(10^{-1})$ in the range $10 < Re < 100$. So, it can be a modest-to-significant correction for laminar two-phase flows.

Similarly, we can show that E_1 and $\alpha_{F,1}$ might be significant compared to other terms in the energy and species continuity equations or, equivalently, the normalized quantities can be $O(10^{-1})$ or higher. The results to the same order of accuracy as cited for Eq. (A.7) are

$$\frac{E_1}{\bar{u}\bar{h}} = -\frac{\overline{u'T'}}{U_0 T_0} = -\frac{2\dot{m}L_{\text{eff}}}{\pi R^2 \rho U_0 c_p T_0 C_D}\frac{\overline{u'u'}}{U_0^2} \tag{A.8}$$

and

$$\frac{\alpha_{F,1}}{\bar{u}\overline{Y}_F} = -\frac{\overline{u'Y'_F}}{U_0 \overline{Y}_F} = \frac{2}{C_D}\frac{A}{\pi R^2}\frac{\overline{u'u'}}{U_0^2} \tag{A.9}$$

For typical fuels and the conditions cited above, we can estimate the coefficients in these last two equations. $E_1/(\bar{u}\bar{h})$ is usually somewhat larger in magnitude than $\overline{u'u'}/U_0^2$ and can be an $O(10^{-1})$ quantity. $\alpha_{F,1}/(\bar{u}\overline{Y}_F)$ has even larger magnitude and should be considered as an $O(10^{-1})$ or higher quantity. So, their importance is demonstrated.

References

Archambault, M.R., Edwards, C.F., MacCormack, R.W., 2003a. Computation of spray dynamics by moment transport equations. I. Theory and development. Atomization Spray. 13, 63–87.

Archambault, M.R., Edwards, C.F., MacCormack, R.W., 2003b. Computation of spray dynamics by moment transport equations. II. Application to calculation of a quasi-one-dimensional spray. Atomization Spray. 13, 89–115.

Bear, J., 1972. Dynamics of Fluids in Porous Media. American Elsevier.

Boivin, M., Simonin, O., Squires, K.D., 1998. Direct numerical simulation of turbulence modulation by particles in isotropic turbulence. J. Fluid Mech. 375, 235–263.

Bulthuis, H.F., Prosperetti, A., Sangani, A.S., 1995. Particle stress in disperse two-phase potential flow. J. Fluid Mech. 294, 1–16.

Courant, R., Hilbert, D., 1962. Methods of Mathematical Physics, vol. 2. Interscience.

Crocco, L., Cheng, S.I., 1956. Theory of Combustion Instability in Liquid Propellant Rocket Motors. Butterworths.

Crocco, L., Harrje, D.T., Reardon, F.H., 1962. Transverse combustion instability in liquid propellant rocket motors. ARS J. 32, 366–373.

Drew, D.A., 1983. Mathematical modeling of two-phase flow. Annual Review of Fluid Mechanics, 15. Annual Reviews, Inc., pp. 261–291.

Drew, D.A., Passman, S.L., 1999. Theory of Multicomponent Fluids. Springer-Verlag.

Druzhinin, O.A., Elghobashi, S., 1998. Direct numerical simulations of bubble-laden turbulent flows using the two-fluid formulation. Phys. Fluids 10, 685–697.

Druzhinin, O.A., Elghobashi, S., 2001. Direct numerical simulation of a three-dimensional spatially developing droplet-laden mixing layer with two-way coupling. J. Fluid Mech. 429, 23–61.
Elghobashi, S., Truesdell, G., 1992. Direct simulation of particle dispersion in decaying isotropic turbulence. J. Fluid Mech. 242, 655–706.
Elghobashi, S., Truesdell, G., 1993. On the two-way interaction between homogeneous turbulence and dispersed solid particles. I. Turbulence modifications. Phys. Fluids 5, 1790–1801.
Ferrante, A., Elghobashi, S., 2003. On the physical mechanisms of two-way coupling in particle-laden isotropic turbulence. Phys. Fluids 15, 315–329.
Fletcher, C.A.J., 1991. Computational Techniques for Fluid Dynamics, vol. II. Springer-Verlag.
Ghosal, S., Moin, P., 1995. The basic equations for the large eddy simulations of turbulent flows in complex geometry. J. Comput. Phys. 118, 24–37.
Givi, P., 2003. Subgrid scale modeling in turbulent combustion: A review. In: Preprint 2003-5081. AIAA.
Gray, W.G., Lee, P.C.Y., 1977. On the theorems for local volume averaging of multiphase systems. Int. J. Multiphase Flow 3, 333–400.
Imaoka, R., Sirignano, W.A., 2003. Vaporization and combustion in three-dimensional droplet arrays. In: Proceedings of the Western States Section/Combustion Institute Fall Meeting. Western States Section/Combustion Institute.
Imaoka, R., Sirignano, W.A., 2004. Vaporization and combustion in three-dimensional droplet arrays. Proc. Combustion Inst. 30, 1981–1989.
Kim, I., Elghobashi, S.E., Sirignano, W.A., 1995. Unsteady flow interactions between an advected cylindrical vortex and a spherical particle. J. Fluid Mech. 288, 123–155.
Kim, I., Elghobashi, S.E., Sirignano, W.A., 1997. Unsteady flow interactions between a pair of advected vortex tubes and a rigid sphere. Int. J. Multiphase Flow 23, 1–23.
Labowsky, M., 1980. Calculation of burning rates of interacting fuel droplets. Combust. Sci. Technol. 22, 217–226.
Ling, W., Chung, J.N., Troutt, T.R., Crowe, C.T., 1999. Direct numerical simulation of a three-dimensional temporal mixing layer with particle dispersion. J. Fluid Mech. 358, 61–85.
Marble, F.E., 1970. Dynamics of dusty gases. Annual Review of Fluid Mechanics, 2. Annual Reviews, Inc., pp. 397–446.
Masoudi, M., Sirignano, W.A., 1997. The influence of an advecting vortex on the heat transfer to a liquid droplet. Int. J. Heat Mass Transfer 40, 3663–3673.
Masoudi, M., Sirignano, W.A., 1998. Vortex interaction with a translating sphere in a stratified temperature field. Int. J. Heat Mass Transfer 41, 2639–2652.
Masoudi, M., Sirignano, W.A., 2000. Collision of a vortex with a vaporizing droplet. Int. J. Multiphase Flow 26, 1925–1949.
Piomelli, U., 1999. Large-eddy simulation: Achievements and challenges. Progr. Aerosp. Sci. 35, 335–362.
Prosperetti, A., Jones, A.V., 1984. Pressure forces in disperse two-phase flow. Int. J. Multiphase Flow 10, 425–440.
Prosperetti, A., Zhang, D.Z., 1995. Finite-particle-size effects in disperse two-phase flows. Theor. Comput. Fluid Dynamics 7, 429–440.
Sankaran, V., Menon, S., 2002a. LES of spray combustion in swirling flows. J. Turbulence 3, 001.
Sankaran, V., Menon, S., 2002b. Vorticity-scalar alignments and small-scale structures in swirling spray combustion. Proc. Combust. Inst. 29, 577–584.
Sirignano, W.A., 1972. Introduction to analytical models of high frequency combustion instability. In: Harrje, D.T., Reardon, F.H. (Eds.), Liquid Propellant Rocket Combustion Instability, NASA SP194. U.S. Government Printing Office, pp. 167–170.
Sirignano, W.A., 1986. The formulation of spray combustion models: Resolution compared to droplet spacing. J. Heat Transfer 108, 633–639.
Sirignano, W.A., 1999. Fluid Dynamics and Transport of Droplets and Sprays. Cambridge University Press.
Slattery, J.C., 1967. Flow of viscoelastic fluids through porous media. AIChE J. 13, 1066–1071.
Soo, S.L., 1967. Fluid Dynamics of Multiphase Systems. Blaisdell.
Spalding, D.B., 1980. Numerical computation of multiphase flow and heat transfer. In: Taylor, C., Morgan, K. (Eds.), Recent Advances in Numerical Methods in Fluids, vol. 1. Pineridge Press, Limited, pp. 139–166.
Squires, K.D., Eaton, J.K., 1991. Preferential concentration of particles by turbulence. Phys. Fluids 3, 1169–1178.

Umemura, A., Ogawa, A., Oshiwa, N., 1981a. Analysis of the interaction between two burning droplets. Combust. Flame 41, 45–55.

Umemura, A., Ogawa, A., Oshiwa, N., 1981b. Analysis of the interaction between two burning droplets with different sizes. Combustion and Flame 43, 111–119.

Wallis, G.B., 1969. One-dimensional Two-phase Flow. McGraw-Hill.

Wang, Q., Squires, K.D., 1996. Large eddy simulation of particle-laden turbulent channel flow. Phys. Fluids 8, 1207–1223.

Whitaker, S., 1966. The equations of motion in porous media. Chem. Eng. Sci. 21, 291–300.

Whitaker, S., 1967. Diffusion and dispersion in porous media. AIChE J. 13, 420–427.

Whitaker, S., 1973. The transport equations for multi-phase systems. Chem. Eng. Sci. 28, 139–147.

White, F.M., 1991. Viscous Fluid Flow, second ed. McGraw-Hill, New York.

Williams, F.A., 1962. Introduction to analytical models of high frequency combustion instability. In: Eighth Symposium (International) on Combustion. Williams and Wilkins, pp. 50–69.

Williams, F.A., 1985. Combustion Theory, second ed. Benjamin Cummings, Reading, MA.

Zhang, D.Z., Prosperetti, A., 1994a. Averaged equations for inviscid disperse two-phase flow. J. Fluid Mech. 267, 185–219.

Zhang, D.Z., Prosperetti, A., 1994b. Ensemble phase-averaged equations for bubbly flows. Phys. Fluids 6, 2956–2970.

Zhang, D.Z., Prosperetti, A., 1997. Momentum and energy equations for disperse two-phase flows and their closure for dilute suspensions. Int. J. Multiphase Flow 23, 425–453.